Strength Analyses of the Weeks Island Bulkheads

Mark L. Blanford and Daniel J. Segalman
Applied Mechanics Division I

R. Leon Parrish
SPR Geotechnical Division

Sandia National Laboratories
Albuquerque, New Mexico 87185

Abstract

When the Morton Salt mine in Weeks Island, Louisiana was converted into a Strategic Petroleum Reserve oil reservoir, massive concrete bulkheads were installed to seal the access shafts against oil or water leakage. Recent inspection of these bulkheads has raised questions about their ability to perform satisfactorily in the event of a catastrophic water leak into the mine. Calculations are reported here which examine the reponse of the five bulkheads to a worst-case scenario of flooding by brine from the surface into the oil reservoir below the bulkheads. These calculations show that, under conservative analysis assumptions, factors of safety under such a load for the bulkheads sealing the service shaft and the two raisebores are close to 1. The Markel incline and production shaft bulkheads exhibit safety factors in excess of 2 and 3, respectively.

Contents

`

Figures

Tables

1. Introduction

Weeks Island, near New Iberia, Louisiana, has been mined for salt since the turn of the century. In 1976 the U.S. Department of Energy (DOE) purchased the Weeks Island mine for crude oil storage as part of the national Strategic Petroleum Reserve (SPR). The mine had two levels, at 500- and 700-ft nominal depths, connected to the surface by two shafts: the production shaft and the service shaft. To allow rapid conversion of the mine to an oil storage facility without undue interruption of salt production, an interim salt mine was developed northwest of the SPR facility, at the depth of the original upper level. Heavy equipment was moved to this interim Markel mine by way of an incline driven from the SPR lower level. During the transition and conversion efforts, two 6-ft boreholes (Raisebore No. 1 and No. 2) were excavated between the Markel access drifts and the SPR lower level.

Before crude oil could be stored in the SPR facility, all access openings had to be sealed. Massive concrete bulkheads were installed in each of the five openings: the production shaft, the service shaft, the Markel incline, and the two raisebores. The location of these bulkheads is shown in Figures 1.1 and 1.2. The bulkheads each consist of a thick concrete lower section, a six-inch layer containing a chemical seal ring (CSR) material, and a second, thinner concrete upper section. The bulkheads were designed both to withstand an explosion in the cavern and to seal against water flooding from the surface. The mine conversion efforts were completed and oil fill commenced in the fall of 1980. The construction history of the mine and conversion details are more fully treated in References [1] and [2].

A visual inspection of the bulkheads several years later revealed radial cracks in the raisebore bulkheads and a circumferential crack in the production shaft bulkhead. In early 1988 DOE asked Jacobs Engineering Group to evaluate the integrity and pressure retention capabilities of the bulkheads. In July 1988 Jacobs submitted a report [3] which concluded that the visible cracks probably indicated structural failure of the upper concrete portion of the bulkheads due to pressure exerted by the CSR material. Sandia participated in a review of this report. Because of the significant cost and risk involved in the proposed upgrades, DOE decided to pursue further testing and analysis before committing to the upgrades.

1.1 Testing Program

Testing revealed that the CSR material, which expands when wet, could generate a pressure of up to 280 psi in a confined space. By coring through the upper bulkhead section of Raisebore No. 1 to the CSR layer, the chemical seal was in fact found to be
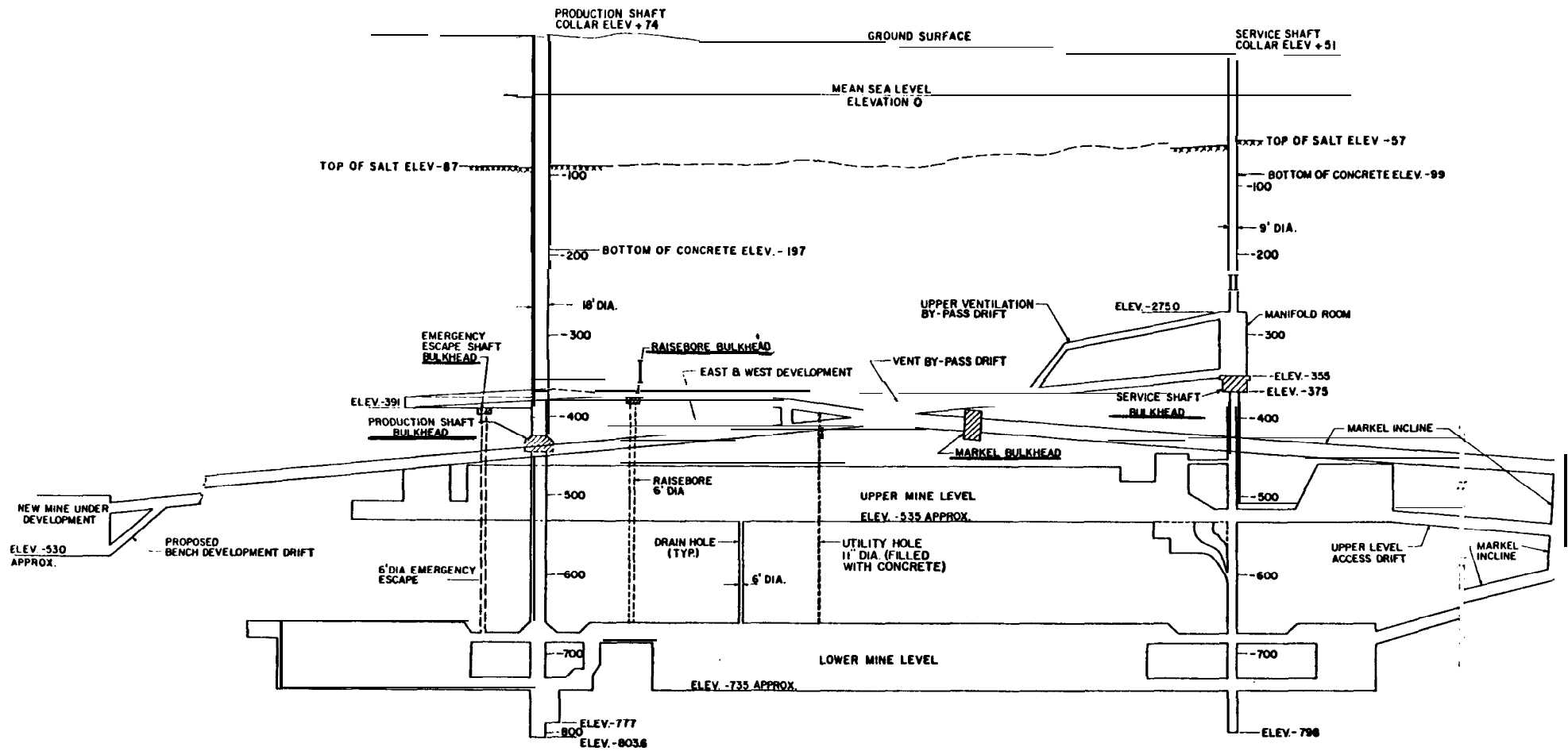
∞

Figure 1.1. Schematic Sectional Elevation of Oil Storage Area, Drifts, and Markel Mine, Showing Location of Five Bulkheads (from Reference [2])
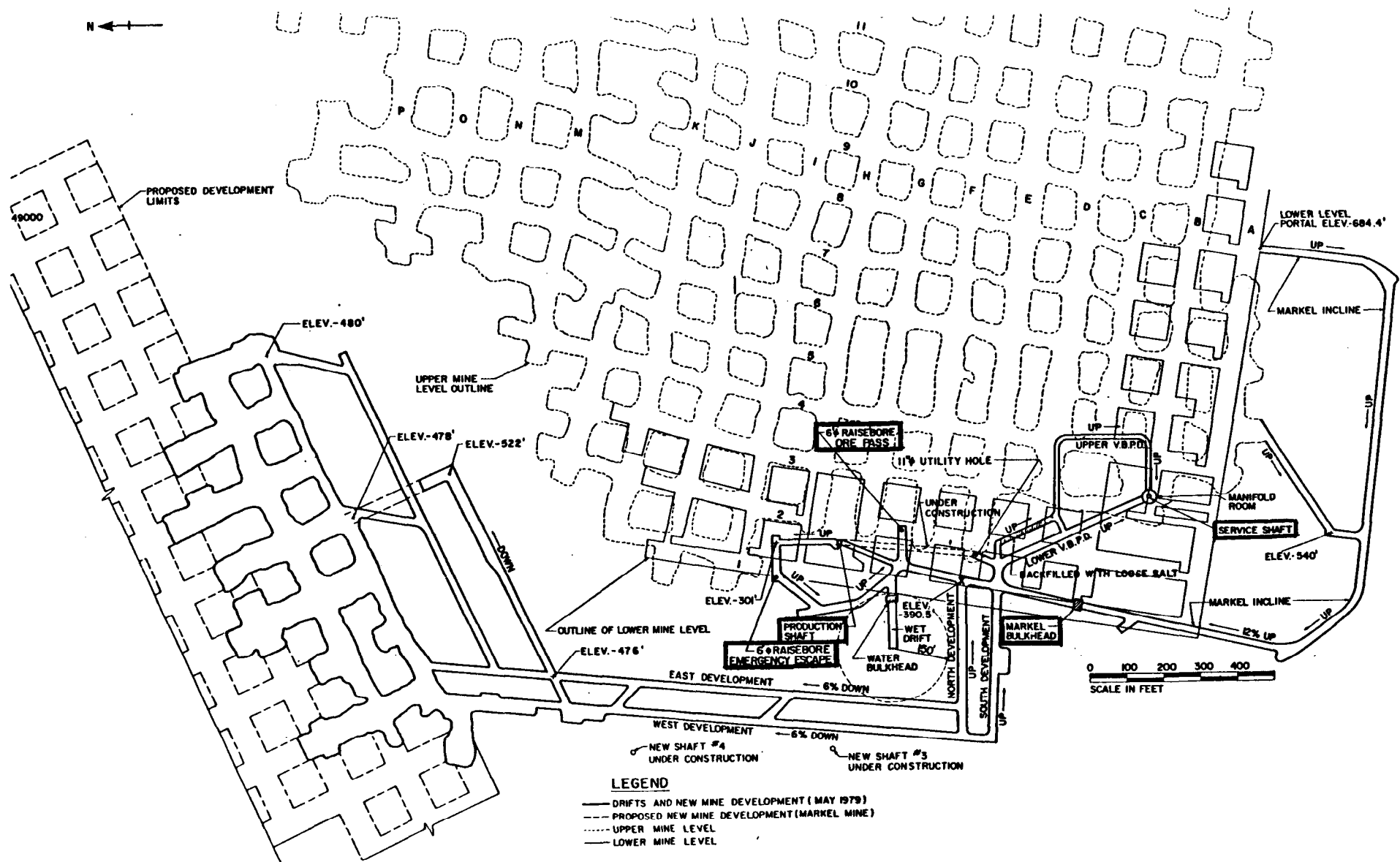
Figure 1.2. Plan of Drifts and Markel Mine (from Reference [2])

under great pressure. Later measurements in the other bulkheads indicated CSR pressure to be 200 psi in Raisebore No. 2, 100 psi in the service shaft, 95 psi in the production shaft, and less than 60 psi (the lower limit of test sensitivity) in the Markel incline. The CSR pressure in Raisebore No. 1 was assumed to have been around 200 psi [4].

Uniaxial compressive tests were conducted on concrete core from the bulkheads. The 28-day design strength of the concrete had been specified at 3000 psi; current unconfined compressive strength averaged 8800 psi [5]. Tests were also proposed to measure the in situ confining stress acting on the bulkheads, but were not performed.

1.2 Analysis Program

Detailed analyses of all the bulkheads were performed by Sandia's Engineering Analysis Department in parallel with Jacobs' consultant, Science and Technology Institute (STI), Inc. Preliminary studies considered loading from the CSR pressure, flooding of the rooms above the bulkheads, and flooding of the oil storage rooms below the bulkheads. Because of differing analysis assumptions and approaches, analysis results varied widely between the two analysis teams. These studies did show, however, that all the bulkheads are most vulnerable to flooding pressure from below which, incidentally, was not considered in the original design criteria.

In August 1989 analysts from Sandia and STI met and reached a technical consensus on major analysis parameters. Models were established for calculating the safety factor of each bulkhead. Specific procedures were also prescribed for incorporating in situ confining pressure into the analyses. Furthermore, material properties and loading conditions were specified. Based on the consensus, each team ran a new set of calculations and met to compare results. In the production and service shaft bulkhead analyses, factors of safety calculated by the two groups still differed by a factor of two. Additional calculations revealed that the discrepancy was due to different numerical treatments of the frictional interface between the bulkheads and the salt mass. Furthermore, the bulkhead stresses were found to be very sensitive to convergence tolerance and domain idealization in two of the nonlinear analysis codes which Sandia used initially [6]. This sensitivity is not present in ABAQUS, the code used to calculate the finite-element results reported here.

This report contains the Sandia analyses of the Weeks Island bulkheads. The analysis approach is explained in Chapter 2. Chapters 3 through 5 document the finite-element calculations for bulkheads in the production shaft, service shaft, and Markel incline, respectively. Closed-form solutions for stresses in the raisebore bulkheads are developed in Chapter 6. Finally, the conclusions drawn from these analyses are restated in Chapter 7.

2. Analysis Approach

In the following discussion it may be helpful to refer to Figure 2.1 which illustrates the configuration of a generic bulkhead. In some instances the reader may also wish to scan drawings of the actual bulkheads. These are presented as the initial figure in each of the next four chapters, respectively.

Preliminary analyses showed that all the bulkheads were most vulnerable to pressures from below, and hence bulkhead failure conditions were developed based on this scenario. The failure of the bulkhead represents a condition in which it cannot perform its intended function and allows oil to escape.

It is feasible to develop modeling methods to determine the pressure at which oil would actually escape through the bulkheads. Such models would require full **three-** dimensional analyses with salt modeled as an elastic/creeping medium and in contact with the precracked upper bulkhead. While the results of such an analysis may be interesting, the technical teams decided that these results would not be pertinent to the rework decision. Instead, reworking of the bulkheads was felt to be necessary if any one of the following conditions is reached due to a simulated flood:

- The bulkhead slabs crack through the thickness direction.

- Rockbolts, where present, yield under calculated loads or the bearing stresses of the bolts on the salt are excessive. In calculating the bearing stresses, creep of the salt would have to be considered.

- A bulkhead key, if present, fails due to inadequate concrete strength.

The stress that would cause one of these conditions, divided by the maximum calculated stress due to the hypothesized flood, defines the factor of safety for a bulkhead.

2.1 Loading and Boundary Conditions

The postulated worst-case loading occurs when a brine leak penetrates the bottom of the oil storage cavern. While the possibility of such a leak occuring in a quiet, stable mine is admittedly remote, it is conceivable that blasting from nearby mining operations or salt movement due to creep or domal activity could initiate a water seep. If such a seep were to connect a fracture zone between the oil storage cavern and a region of the salt dome having hydraulic connectivity to the surface, meteoric brine may begin seeping into the SPR facility. As schematically diagramed in Figure 2.2, the brine head
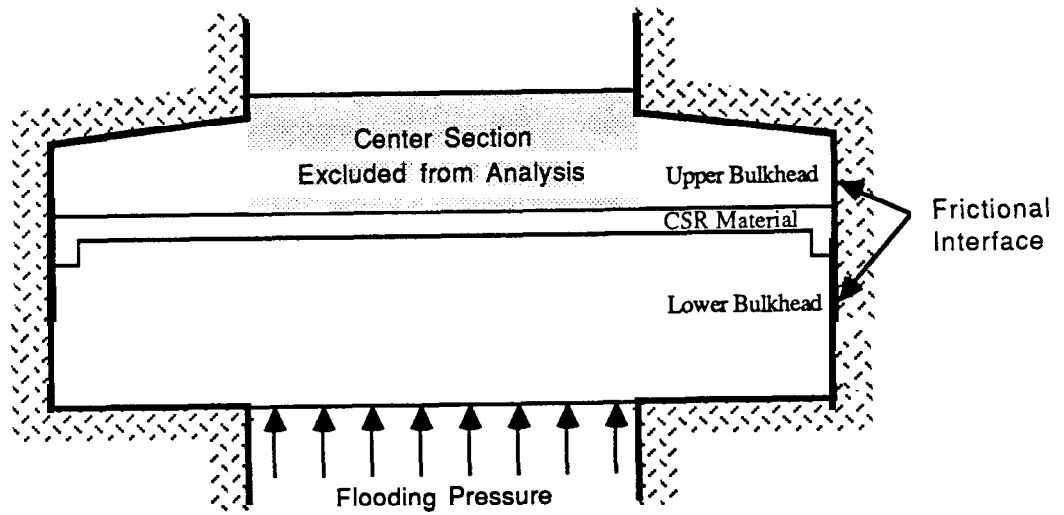
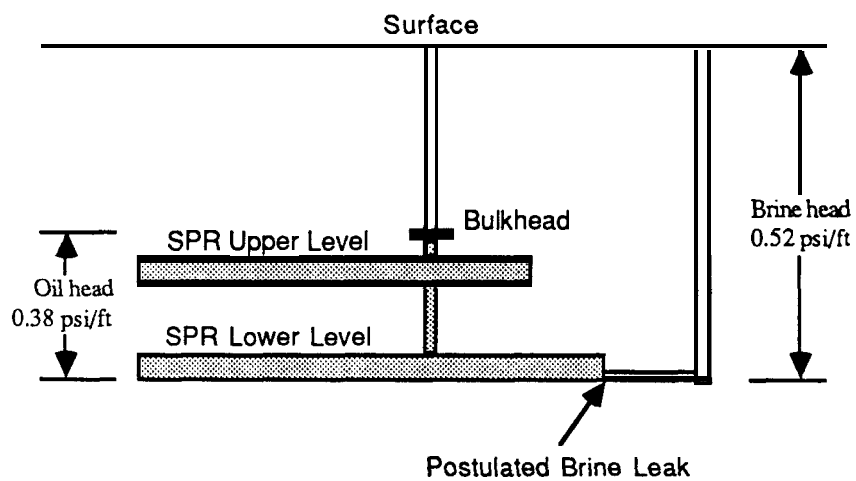**Figure 2.1.** Configuration of a Generic Bulkhead

Figure 2.2. Schematic Diagram of SPR Facility for Calculation of Flooding Pressure

Table 2.1. Uplift Pressure Acting on Bulkheads from Flood Scenario

Bulkhead	Elevation	Fluid Pressure	Adjusted Pressure
Production Shaft	-445 ft	276 psi	256 psi
Service Shaft	-375 ft	250 psi	230 psi
Markel Incline	-421 ft	267 psi	267 psi
Raisebore No. 1	-375 ft	250 psi	240 psi
Raisebore No. 2	-390 ft	255 psi	245 psi

was calculated from six feet above mean sea level extending down 750 ft. The pressure acting on each bulkhead from this flood would be the weight of the brine column minus the weight of the oil column from the leak point to the lower surface of the bulkhead. In the analyses, this pressure has been adjusted to account for the weight of the bulkhead where appropriate. Table 2.1 shows the results of this calculation for each bulkhead. These values were used by both analysis teams.

All parties agreed that it was not appropriate to consider dynamic loading effects (i.e., momentum effects) for this flooding scenario, for the following reasons. First, if underground water leaks occur, they start small and increase gradually over a period of days or months as the salt is leached away. Second, the large volume of trapped air in the storage cavern would act as a cushion for any sudden increase in fluid volume. It would take quite a large volume of additional fluid to enter the cavern for there to be an appreciable increase in pressure. This could only happen over an extended period of time.

To prepare for the installation of each bulkhead, the shaft or drift at that location was first widened using a Continuous Miner. Concrete was then poured to fill the enlarged opening. To prevent solutioning of the salt walls by the fresh-water concrete mix, the salt surfaces were painted with sodium silicate and allowed to dry beforehand. The resulting interface between the concrete and salt was thus thought to be relatively weak. The analysis groups agreed to idealize the interface using a Coulomb friction model with friction coefficient of 0.1. In this model shear tractions are allowed to reach ten percent of the normal tractions before any relative movement occurs across the interface. Any additional shear load is relieved by sliding at the interface, and no further increases in the shear tractions occur. The interface is modeled with zero tensile strength. Proper numerical treatment of this nonlinear, path-dependent interface turned out to be an important factor in arriving at consistent predictions of the stresses in the bulkhead.'

The friction coefficient of 0.1 was chosen as a conservative lower bound. Measurements of friction coefficients in laboratory tests indicate that this lower bound may be

---

[1] For instance, when the Markel incline bulkhead was reanalyzed using a friction coefficient of 0.2, the predicted factor of safety rose by 20 percent.

ultra-conservative. In fact, coefficients of friction in the range **0.1** to **0.2** are typical of laboratory tests where smoothly-cut salt core is in contact with highly-polished stainless steel platens (see Wawersik [7]). Moreover, the lower friction coefficents in that study were obtained by introducing a lubricant film of molybdenum disulfide on the interface. In a personal communication, Wawersik indicated that it would be possible to measure the actual salt-concrete interface properties given a sample of core penetrating the interface. From a description of the bulkhead construction sequence, he estimated that the friction coefficient would be minimally 0.4.

The circumference of each bulkhead is under in situ confining pressure caused by the creep of salt around the opening. The original lithostatic stress of 400 psi had been relieved locally due to excavation of the shaft or drift. Since the installation of the bulkheads, confining pressure at the interface has been gradually building up. The extent to which the salt creep has restored the confining pressure is unknown. To avoid the necessity of performing detailed creep calculations, the following elastic model was judged to produce realistic in situ confining stresses around the bulkhead for the time frame of interest.

In the elastic model, salt is assumed initially to occupy the entire modeled region at a uniform hydrostatic stress of 100 psi (one-fourth the original lithostatic stress). Far-field boundaries in the model are fixed against normal displacement. This configuration is in equilibrium. Salt in the shaft or drift is then removed and an initially unstressed concrete bulkhead is emplaced at the same time. A new equilibrium displacement field is sought. In practice, this idealized emplacement scheme was modeled in a single step by meshing only the final configuration (bulkhead in the excavated salt) and applying a 100 psi initial hydrostatic stress field to the salt alone. The first finite-element load step then established equilibrium between the salt, concrete, and shaft or drift. Flooding pressure was subsequently applied.

2.2 Configuration

Visual inspection of the upper surface of the bulkheads has shown that several of them are already cracked. Preliminary analyses indicated that the cracks could be caused by the pressure built up in the CSR material, in which case the damage would be limited to the upper section of the bulkhead. Consequently it is not clear how much structural support the upper bulkhead could contribute in the event of a flood from below. In most of the analyses reported here the central, vulnerable portion of the upper bulkhead was assumed to provide no restraint whatsoever. The upper section of each bulkhead was therefore modeled as only the **annulus** which remained after removing the entire central portion. This assumption is quite conservative, since the upper bulkheads in the raisebore shafts have demonstrated the capacity to withstand substantial CSR pressure, even when cracks may have penetrated the thickness.

Furthermore, if the center section of the upper bulkhead contributed no restraint,

Table 2.2. Elastic Constants Used in Analyses

Material	E	ν
Concrete	4.0×10^6 psi	0.18
Salt	0.378×10^6 psi	0.29

any pressure on the CSR material would be relieved and the CSR material would be extruded into the central opening. This would allow the lower bulkhead to move upward until it rested against the remaining annulus of the upper bulkhead-a translation of approximately 6 inches. The resulting weakened configuration (admittedly hypothetical and quite conservative) served as the basis for the finite-element stress analyses reported here.

2.3 Material Properties

The salt and the concrete were analyzed for their elastic response to a postulated flood. The elastic constants used are given in Table 2.2. The Young's modulus for salt was provided by Jacobs Engineering [3] basedon measurements performed on core samples.

The safety factor is defined as the strength of the material divided by the calculated maximum stress. Several 4-in diameter core samples from the upper concrete bulkheads were tested in compression. The average unconfined compressive strength was just over 8800 psi [5]. Considering the range of values measured, a strength of $f'_c = 8500$ psi was chosen as being suitably conservative. Following generally-accepted procedures [8], tensile strength was then taken to be $5\sqrt{f'_c} = 461$ psi, a conservative estimate for split-cylinder tensile strength. From the general shape of concrete's failure surface under multiaxial stress states, the direct shear strength was estimated at $6\sqrt{f'_c} = 553$ psi. It is recognized that concrete can withstand substantially more shear stress as the mean compressive stress increases.

The preceeding approach was agreed upon by consensus among **members of the** analysis teams. In the following description of the Sandia analyses, any particular implementation issues **or** remaining assumptions were our own.

3. Production Shaft Bulkhead

The production shaft has a circular cross section with a 9-ft radius. To install the bulkhead, a drift was excavated to intersect the shaft tangentially 30 ft below the Markel-level landing. An Alpine Continuous Miner then widened the shaft to a 20.5-ft radius, spiraling downward until the bulkhead area was excavated to a height of 20 ft [1]. The three-part bulkhead was then placed, as shown in Figure 3.1.
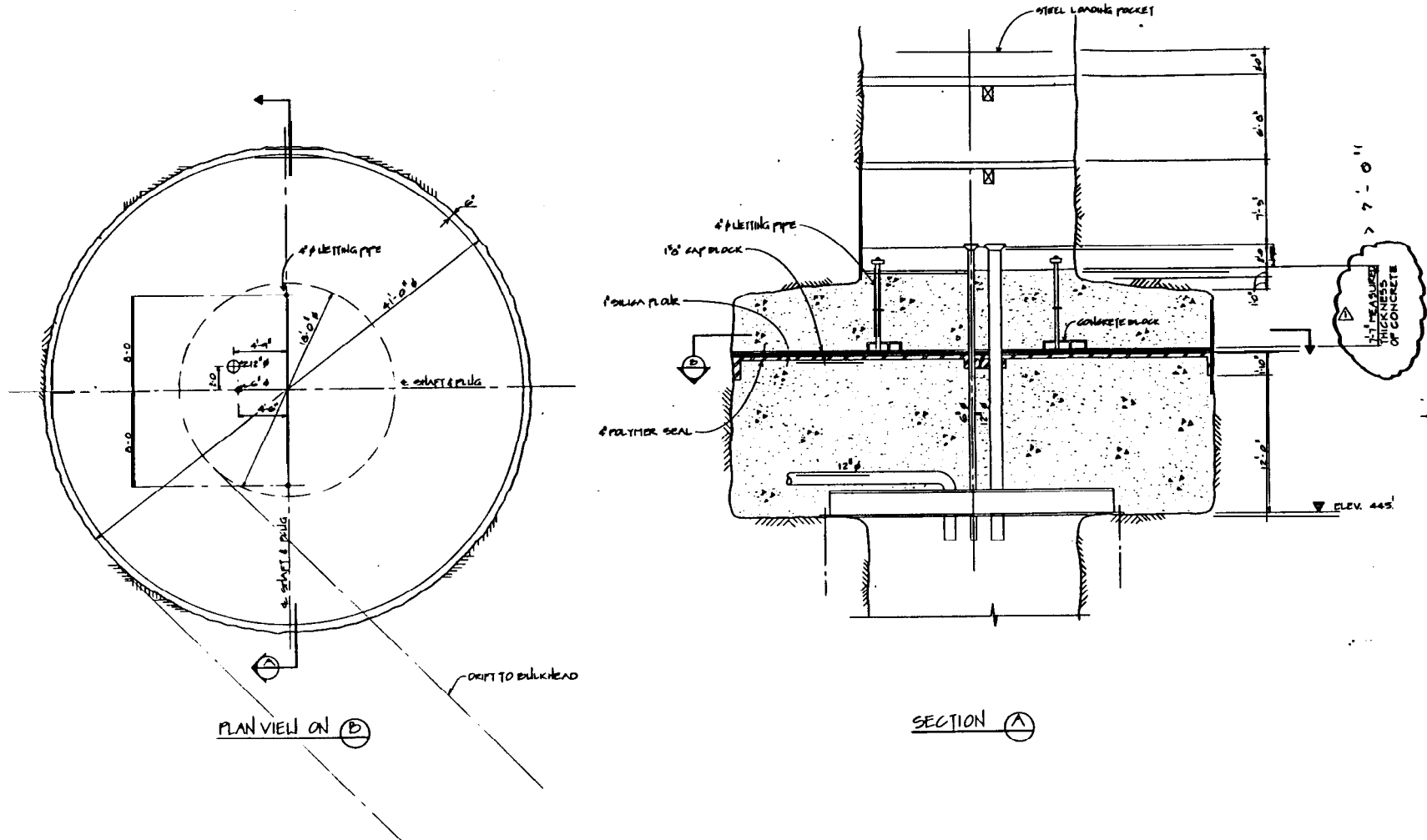
3.1 Model

The bulkhead was modeled taking advantage of the axial symmetry of the geometry and loading. Figure 3.2 shows the finite-element mesh of 783 nodes and 722 elements used to analyze the region. The far-field boundaries are all constrained against displacement normal to the boundary, with the exception of a small area at the top center of the mesh. This area, 40 ft in diameter, was left as a free surface to approximate the presence of the Markel-level landing 30 ft above the bulkhead. (The deformation that occurs at this free surface will be obvious in the deformed mesh plots of Figure 3.3.) As described in Section 2.2, the center of the upper bulkhead has been removed, leaving an annulus of concrete resting against the upper shoulder of the salt. The lower bulkhead has been translated upwards so that it is in contact with the upper annulus.

This configuration was analyzed using the general-purpose nonlinear finite element code ABAQUS [9]. Axisymmetric CAX4 elements were used in the salt and concrete regions, and INTER2A interface elements were used between the salt and concrete and between the upper and lower bulkheads. All the interface elements were assigned a friction coefficient of 0.1. The salt was initialized with a compressive normal stress of 100 psi in all directions.

3.2 Results

The analysis consisted of two load steps as described in Section 2.1. A plot of the deformed mesh in response to these two load steps is shown in Figure 3.3. This figure takes advantage of the symmetry of the problem to display deformations resulting from the initial stresses in the reflected plot on the left side, and deformations from the subsequent flooding pressure on the right. This makes it easier to compare the effects of the two load steps. Deformations have been exaggerated 200 times to aid in visualization. The lower salt shoulder appears to pass through lower bulkhead surface in the left-hand plot, but this is merely an artifact of exaggerating the deformations. In fact, this just indicates that there has been relative closure between the two surfaces. The average radial pressure

PLAN VIEW ON Ⓑ

SECTION Ⓐ

Figure 3.1. As-Built Drawing of Production Shaft Bulkhead
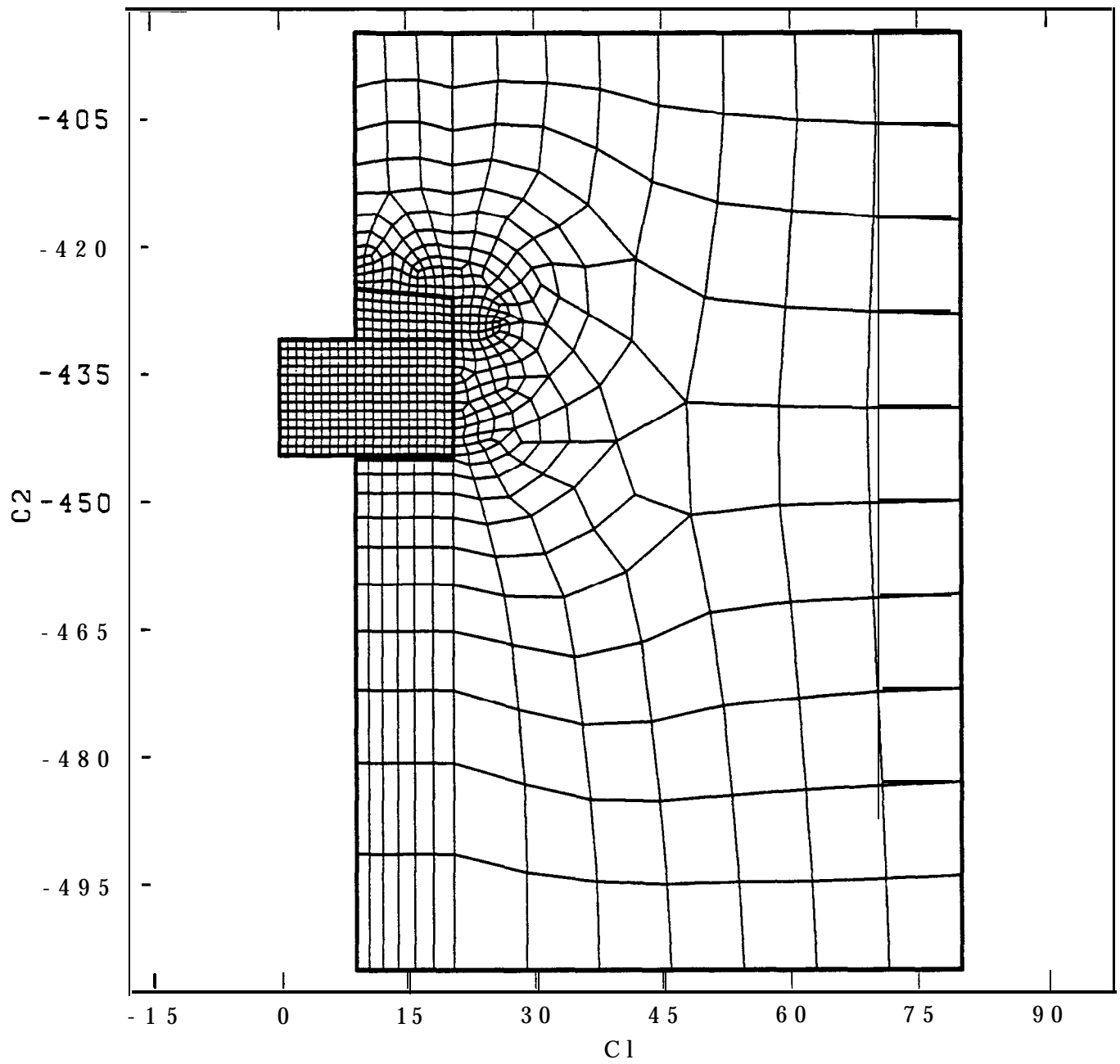
Figure 3.2. Mesh Used in Analyzing the Production Shaft Bulkhead

exerted by the salt onto the lower bulkhead in the first step of this analysis was found to be 92 psi.

The deformations on the right half of Figure 3.3 correspond to a flooding pressure of 256 psi applied to the lower surface of the lower bulkhead and all exposed faces of the salt below the bulkhead. The most severe stress is the radial normal stress caused by bending of the bulkhead. Contours of the radial stress are shown in Figure 3.4. Profiles of the radial and axial stresses through the thickness of the bulkhead are shown in Figure 3.5. These profiles correspond to stresses calculated at the center of Elements **1** through **13** (see Figure 3.3) Compressive axial stresses vary from less than 1 psi in Element 1 near the upper free surface to 254 psi in Element 13 near the flooded surface. Extrapolation of these profiles to the boundaries yields the boundary tractions as expected. Radial bending stresses range from 114 psi tension in Element 1 to 310 psi compression in Element 13. When extrapolated to the upper surface at the center of the bulkhead, the calculated tensile stress reaches a maximum of 149 psi. Compared to the concrete's assumed tensile strength of 461 psi, this results in a safety factor of 3.1.

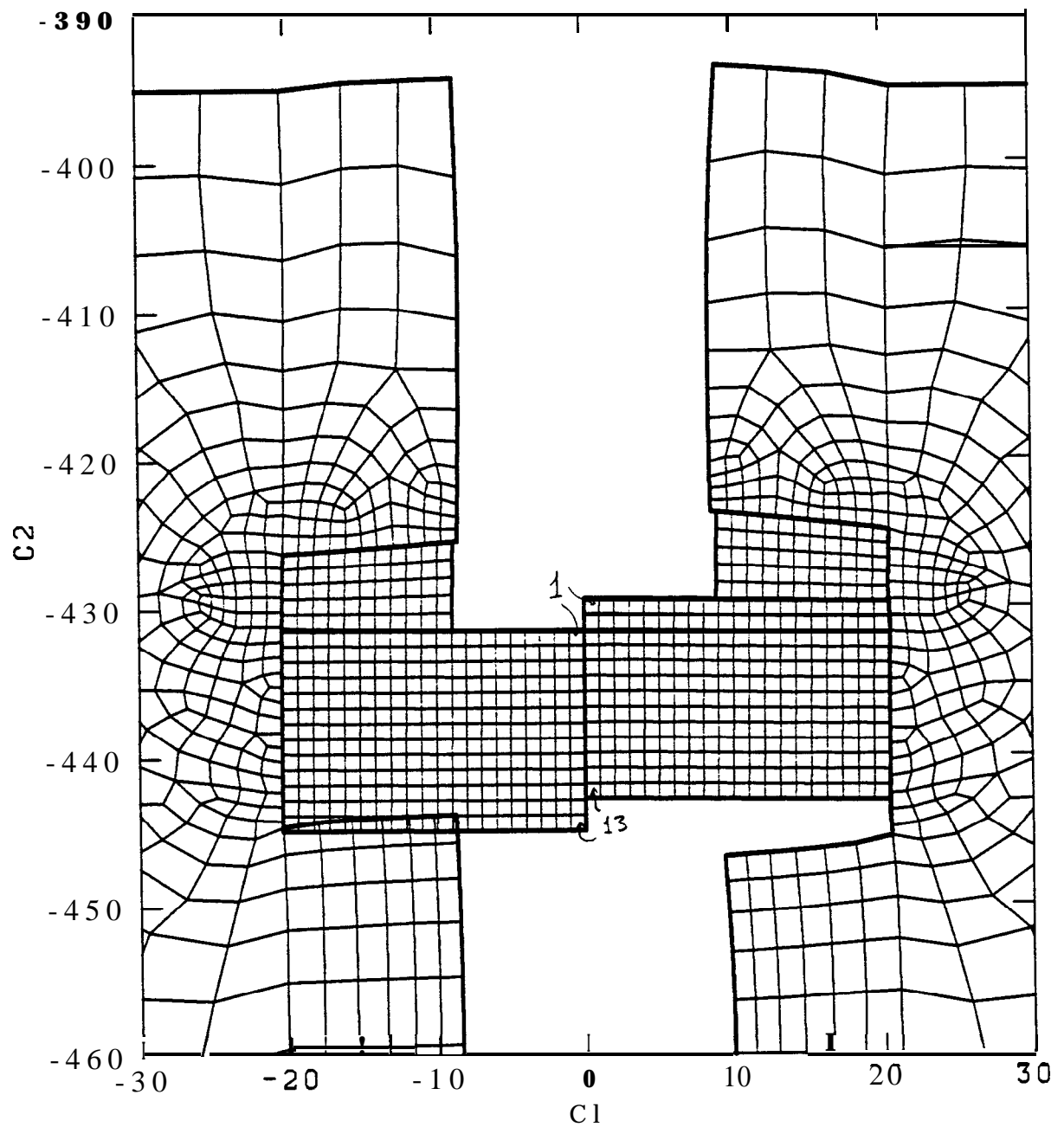**Figure** 3.3. Deformed Mesh of Production Shaft Bulkhead Response to Initial Stress Only (Left) and to Flooding Pressure **as** Well (Right)
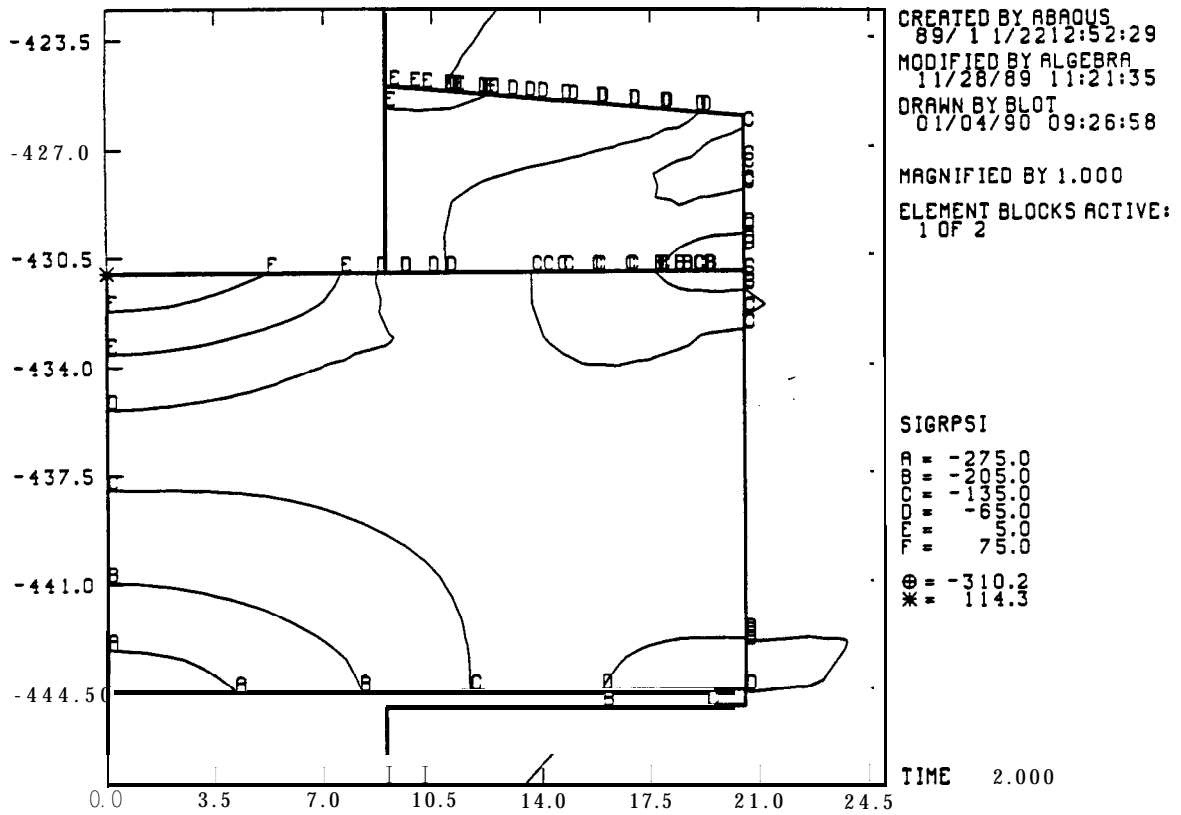
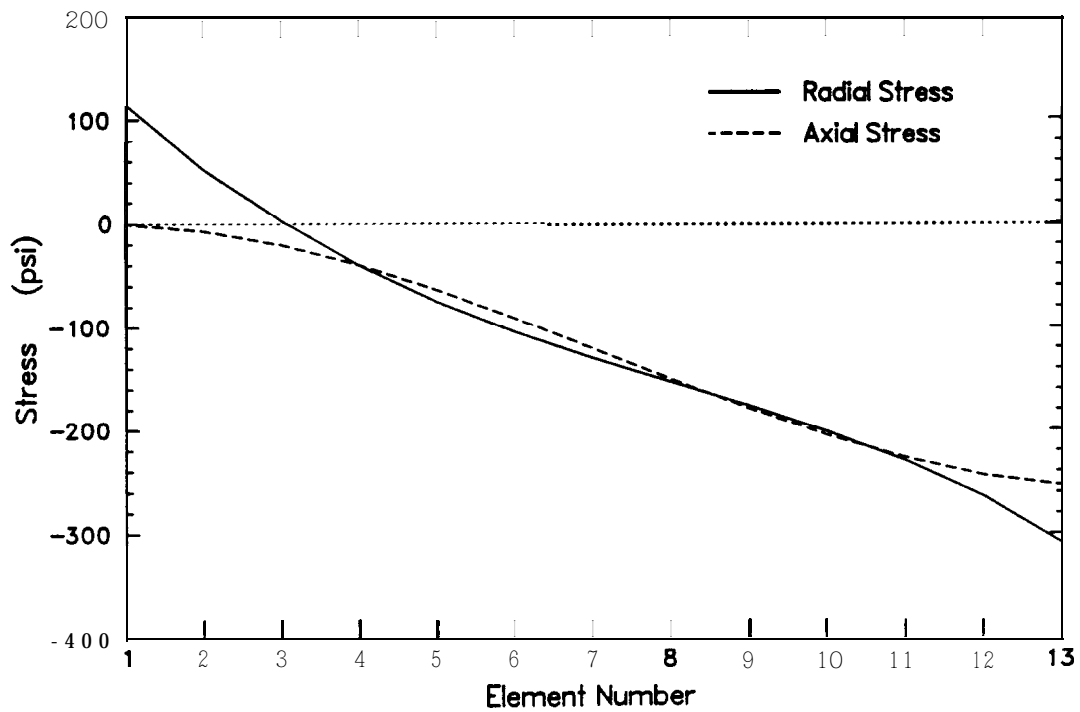**Figure 3.4.** Contours of Radial Stress (SIGRPSI) in Production Shaft Bulkhead

Figure 3.5. Variation of Radial and Axial Stress through the Thickness of the Production Shaft Bulkhead

22

4. Service Shaft Bulkhead

At the depth of the bulkhead, the service shaft is rectangular in cross-section measuring 10 ft by 12 ft. A 100-ft section of the shaft was widened to 40 ft diameter to accommodate pumping equipment. Continuous miners were used to excavate this manifold room to avoid blasting damage to the walls. The service shaft bulkhead was installed in the bottom 20 ft of the room. At an elevation of 355 ft below mean sea level, which was to be the floor of the manifold room, the shaft was even further widened to a finished diameter of 46 ft to a depth of 5.5 ft to provide a keyway as an anchor for the bulkhead.

Figure 4.1 reproduces an as-built drawing of the bulkhead. The bulkhead is perforated with several casings, providing access for process piping and instrumentation into the cavern storage area. These include one 24-inch casing, thirteen 18-inch casings, one 12-inch casing, and six 6-inch casings. These were suspended from a structural steel framework which had been installed on a ledge cut into the shaft wall. The concrete was placed in three lifts: one for the lower bulkhead, and two for the upper bulkhead. This left a cold joint in the upper bulkhead at the level of the central sump area. The cold joint is not shown in Figure 4.1, but will be apparent in the finite element mesh described below. As in the other bulkheads, a layer of CSR material, silica flour, and cap block separate the upper and lower bulkheads. The installation procedure is more fully dealt with in Reference [1].

4.1 Model

The region was modeled using an axisymmetric approximation of the geometry and loading. Figure 4.2 shows the finite-element mesh of 701 nodes and 631 elements used to analyze the region. The far-field boundaries are all constrained against displacement normal to the boundary. The cylindrical approximations chosen to model the shaft below the bulkhead and the cutouts in the bulkheads were selected to give the same circular cross-sectional area as their rectangular counterparts. For simplicity the modeled manifold room extends to the top of the mesh, though in reality the room has a ceiling at -275 ft elevation.

The portion of the mesh representing the bulkhead is expanded in Figure 4.3. Some of the regions in the bulkhead contain irregularly-shaped elements. This was done to help control non-physical "hourglass" deformations of the mesh in some of the preliminary analysis runs. However, the CAX4 elements used in the present analysis are not susceptible to these spurious deformation modes.

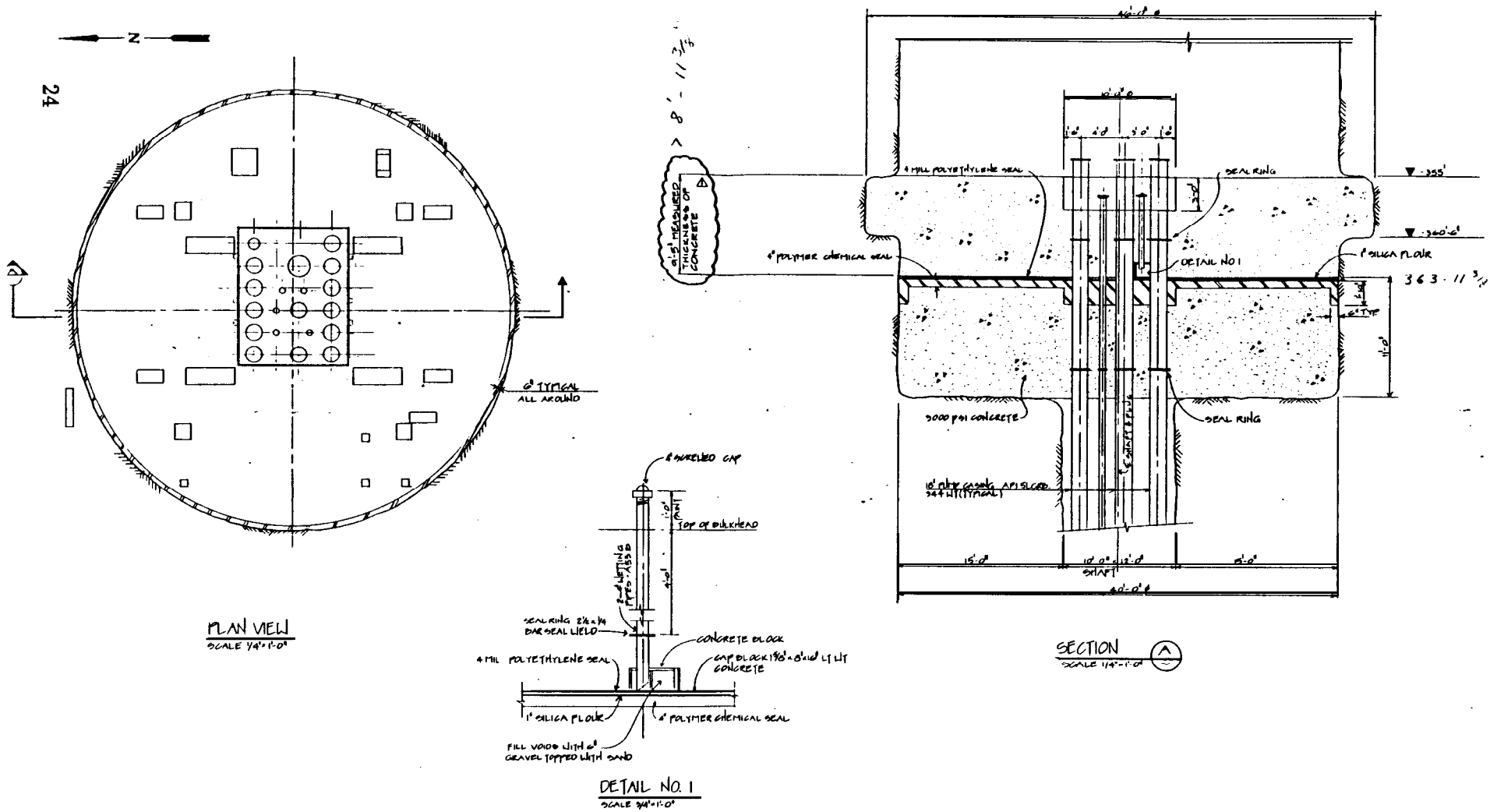As described in Section 2.2, the center of the upper bulkhead was excluded from

Figure 4.1. As-Built Drawing of Service Shaft Bulkhead
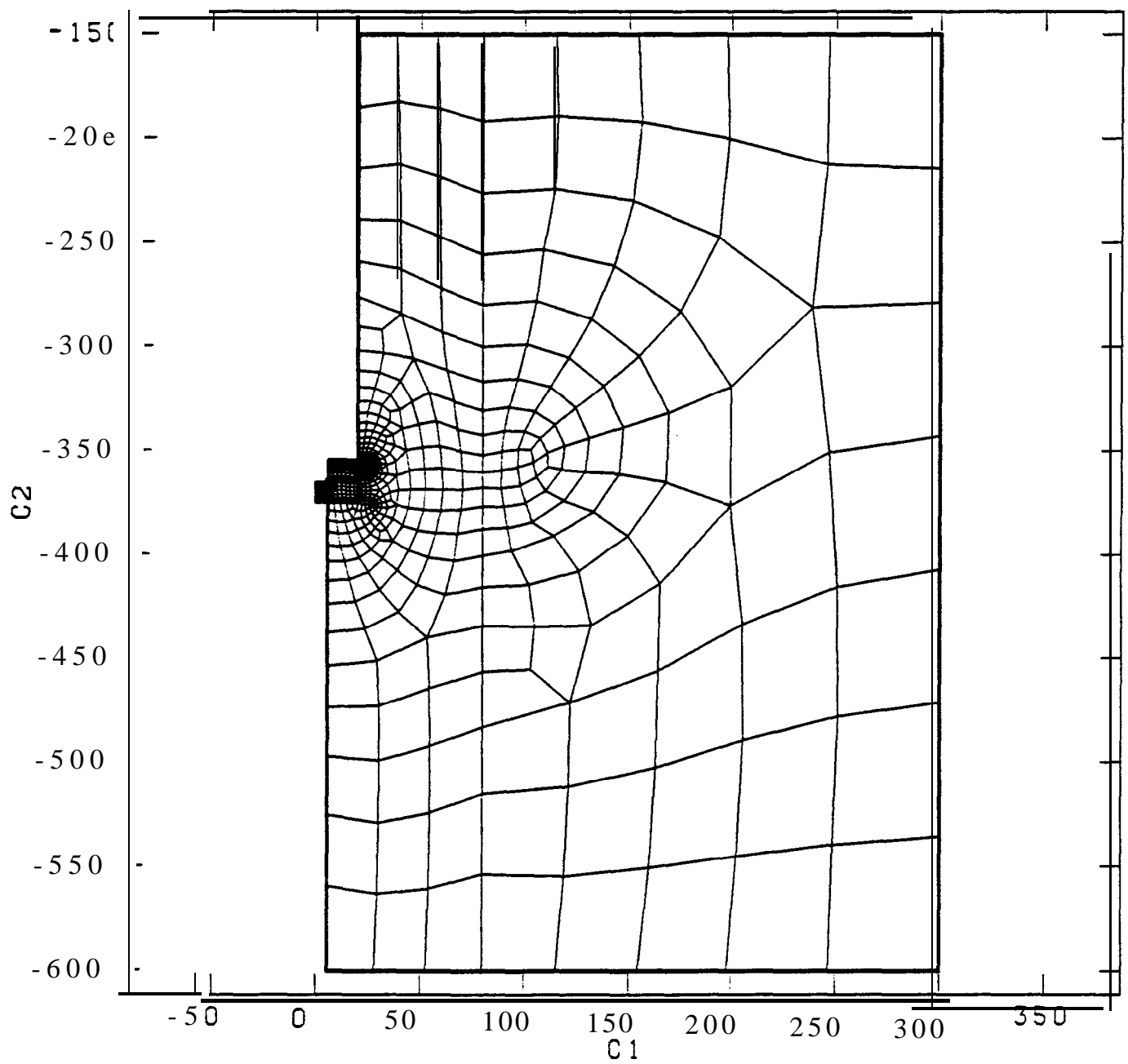
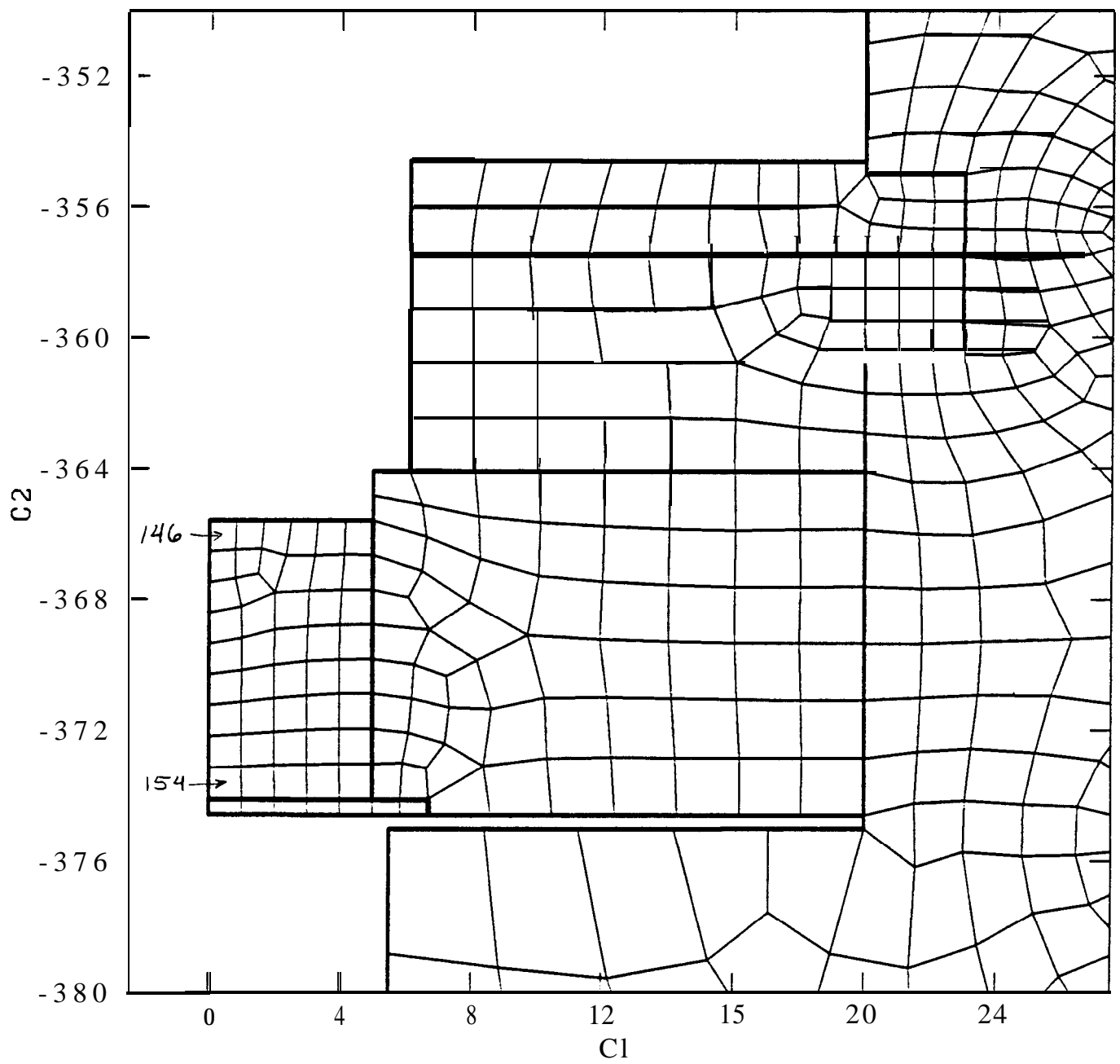Figure 4.2. Mesh Used in Analyzing the Service Shaft Bulkhead

Figure 4.3.   Close-Up of Mesh in the Service Shaft Bulkhead

the model, leaving only an **annulus** of concrete that is keyed into the room wall. This **annulus** is meshed in two sections separated by a horizontal line of interface elements, representing the cold joint between the two lifts of concrete.

The lower bulkhead has been translated upwards so that it rests in contact with the upper **annulus.** Two details of the lower bulkhead model deserve special note. First, the structural steel framework suspending the casings has been explicitly accounted for by including a row of elements at the bottom of the bulkhead with properties of steel ($E = 30 \times 10^6$ psi, $\nu = 0.3$). Second, Young's modulus in the center section of the lower bulkhead was reduced by 36 percent, which is the percentage of the center section volume which is occupied by the casings.

This configuration was analyzed using ABAQUS. Axisymmetric CAX4 elements were used in the salt, concrete, and steel regions, and **INTER2A** interface elements were used between the salt and concrete, between the upper and lower bulkheads, and to represent the cold joint in the upper bulkhead. All the interfaces were assigned a friction coefficient of **0.1** except for the cold joint. The joint was given a coefficient of 0.5 so as to represent the concrete-concrete interface more accurately. The salt mass was initialized with a compressive normal stress of **100** psi in all directions.

4.2 Results

The analysis was accomplished in two load steps, as described in Section **2.1.** A plot of the deformed mesh in response to these two load steps is shown in Figure 4.4. This figure again takes advantage of the symmetry of the problem to display the first load step in the reflected plot on the left side, and the second load step on the right. This makes it easier to compare the effects of the two load steps. Deformations have been magnified 200 times to aid in visualization. Again, the lower salt shoulder appears to pass through lower bulkhead surface in the left-hand plot, but this is merely an artifact of exaggerating the deformations. The average radial pressure exerted by the salt onto the lower bulkhead in the first load step (initial stress only) was found to be 94 psi.

For the second load step, a flooding pressure of 230 psi was applied to the lower surface of the lower bulkhead and all exposed faces of the salt below the bulkhead. The right half of Figure 4.4 shows the resulting deformations. The lower surface of the upper bulkhead **keyway** has been lifted off the salt shoulder; each interface element between the separated surfaces is plotted as an **"×".** Two stresses are of potential concern in this load case: the radial stress in the lower bulkhead due to its bending, and the shear stress in the key of the upper bulkhead.

Contours of radial stress are plotted in Figure 4.5. Stresses in the structural steel framework at the bottom of the lower bulkhead are beyond the range of the contours, reaching 3,200 psi in compression. This is well within the structural capacity of the steel, and is not of interest to us here. Figure 4.6 shows the variation of radial and axial stress
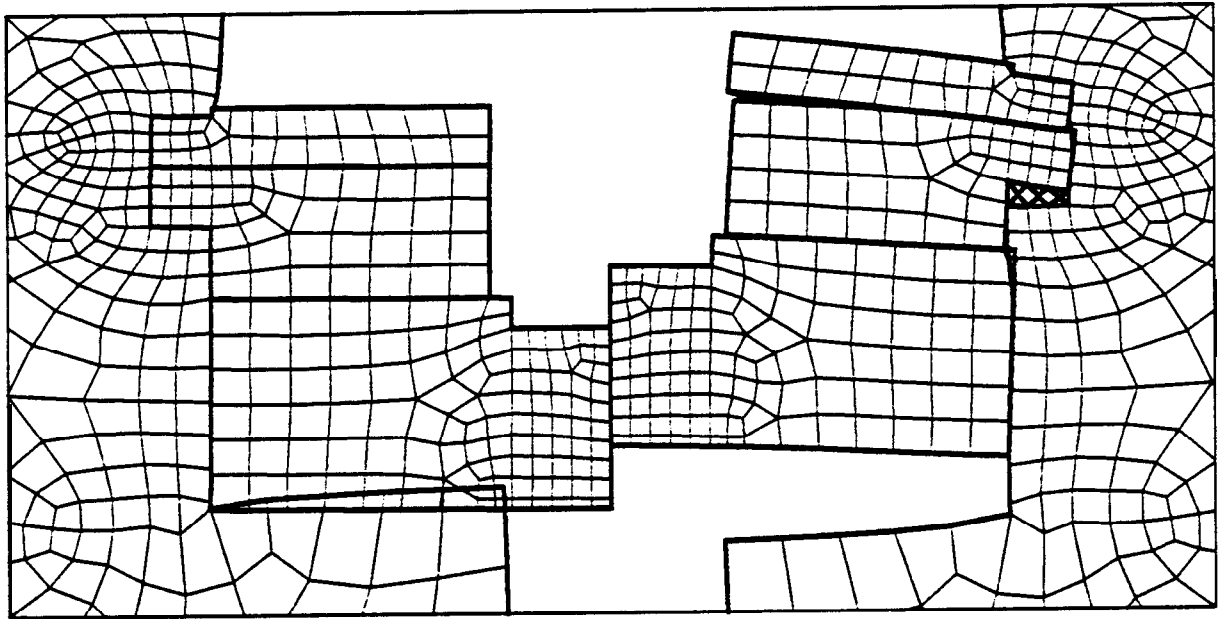
Figure 4.4. Deformed Mesh of Service Shaft Bulkhead Response to Initial Stress Only (Left) and to Flooding Pressure as Well (Right)
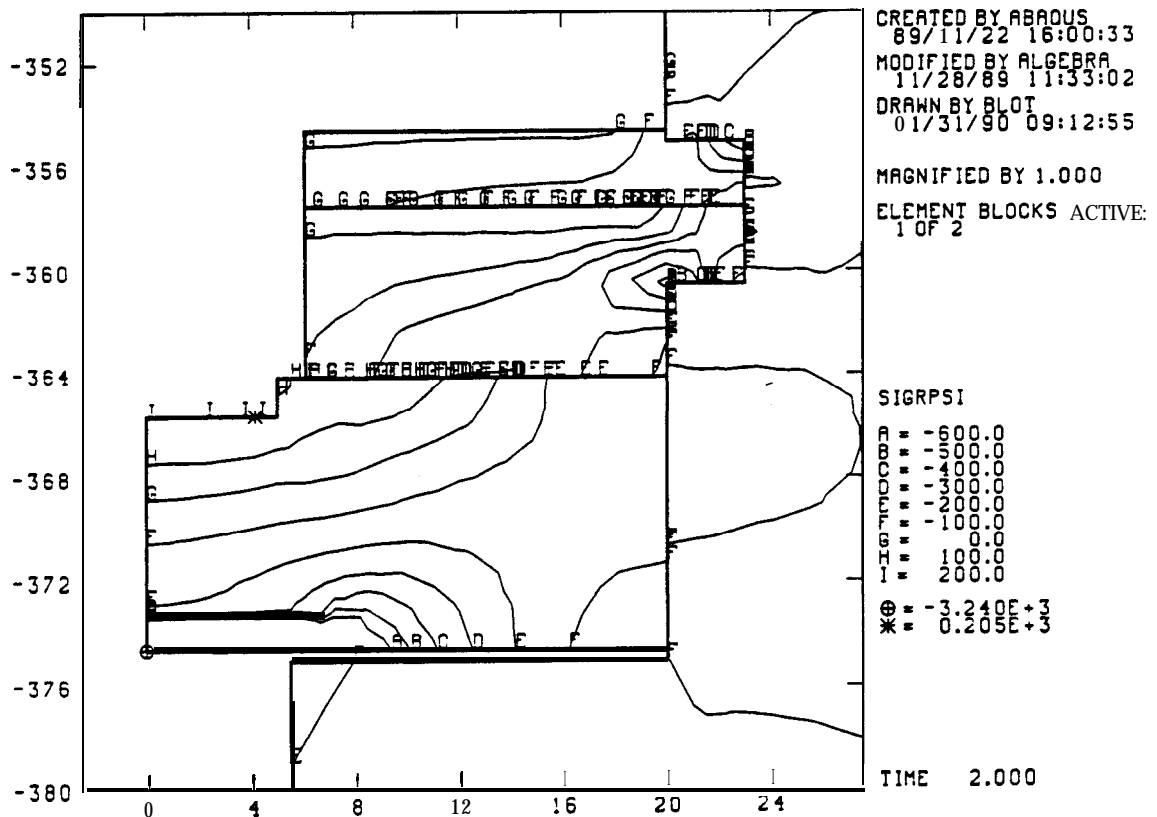
Figure 4.5. Contours of Radial Stress (SIGRPSI) in Service Shaft Bulkhead

through the thickness of the lower bulkhead, up to but not including the structural steel framework at the bottom. The maximum radial tensile stress of just over 200 psi occurs along the top of the cutout area of the lower bulkhead.

To estimate the maximum stresses that would be encountered in the bulkhead under this loading, we must make two adjustments to the 200 psi value obtained from the plot. One accounts for the fact that a reduced stiffness was used to represent an average deformational response of concrete that had been perforated by many casings. To estimate the stress generated in the concrete matrix between the casings, the computed average stress must be scaled upward by the same factor used to scale down the stiffness. This results in an estimated tensile stress in the concrete of 319 psi. The second adjustment is to extrapolate the stress from the centroid of the finite element to the upper surface of the bulkhead. This procedure gives a tensile stress of 370 psi at the surface of the bulkhead. When compared with the assumed concrete tensile strength of 461 psi, the calculated factor of safety due to bending comes to 1.25.

Because the service shaft bulkhead relies on a concrete key to anchor it to the salt, the magnitude of shear stresses generated in the key are a potential concern in the event of flooding from below. Figure 4.7 shows contours of shear stress generated in the bulkhead. This indicates that the maximum shear stresses occur at the base of the key in the upper bulkhead. Although the contour plot indicates that the maximum stress is 396 psi, this is actually the average stress from the three elements adjacent to the corner node. The maximum shear stress calculated at an element centroid is 514 psi, occuring in an element at the base of the key. If this is compared to 553 psi (the assumed strength of concrete at zero mean stress), a safety factor of 1.1 results.

However, the mean stress at the base of the key is not zero, but 538 psi in compression because of bending effects. The shear strength of concrete shows a very strong dependence on the mean stress. A simple Coulomb criterion for the pressure dependence is given by $\tau = c + \sigma \tan \phi$, where τ is the shear strength, c is the cohesion (shear strength at zero mean stress), $\sigma = \frac{1}{3}(\sigma_r + \sigma_z + \sigma_\theta)$ is the mean stress (compression positive), and ϕ is an "angle of internal friction." Having assumed $c = 6\sqrt{f'_c} = 553$ psi, this implies $\phi = 52.5°$ to match the unconfined compressive strength of 8500 psi. With this criterion, and using the maximum tensor shear as a stress measure, we calculate a safety factor of 2.1 in the key. If we conservatively assume that the shear strength is much less sensitive to the mean stress (say $\phi = 30°$) without increasing the cohesion, the safety factor in shear is still above 1.6.

In conclusion, the capacity of the service shaft bulkhead to withstand flooding from below is limited by its resistance in bending. The calculated factor of safety assuming a worst-case set of stresses is 1.25.
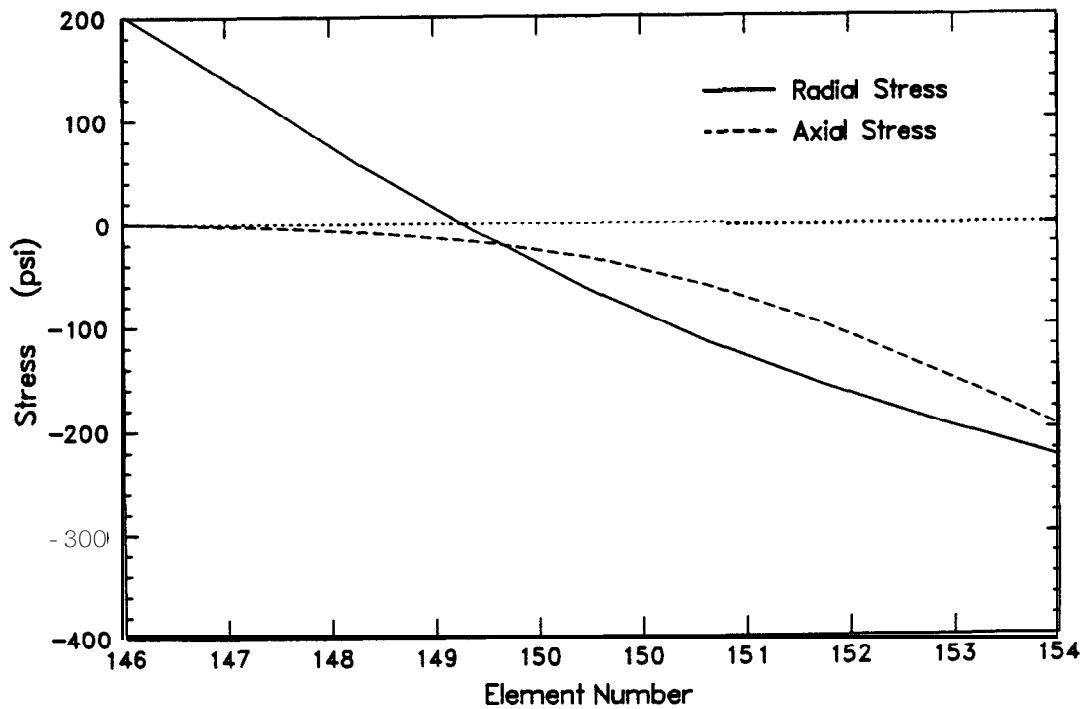
Figure 4.6. Variation of Radial and Axial Stress through the Thickness of the Service Shaft Bulkhead
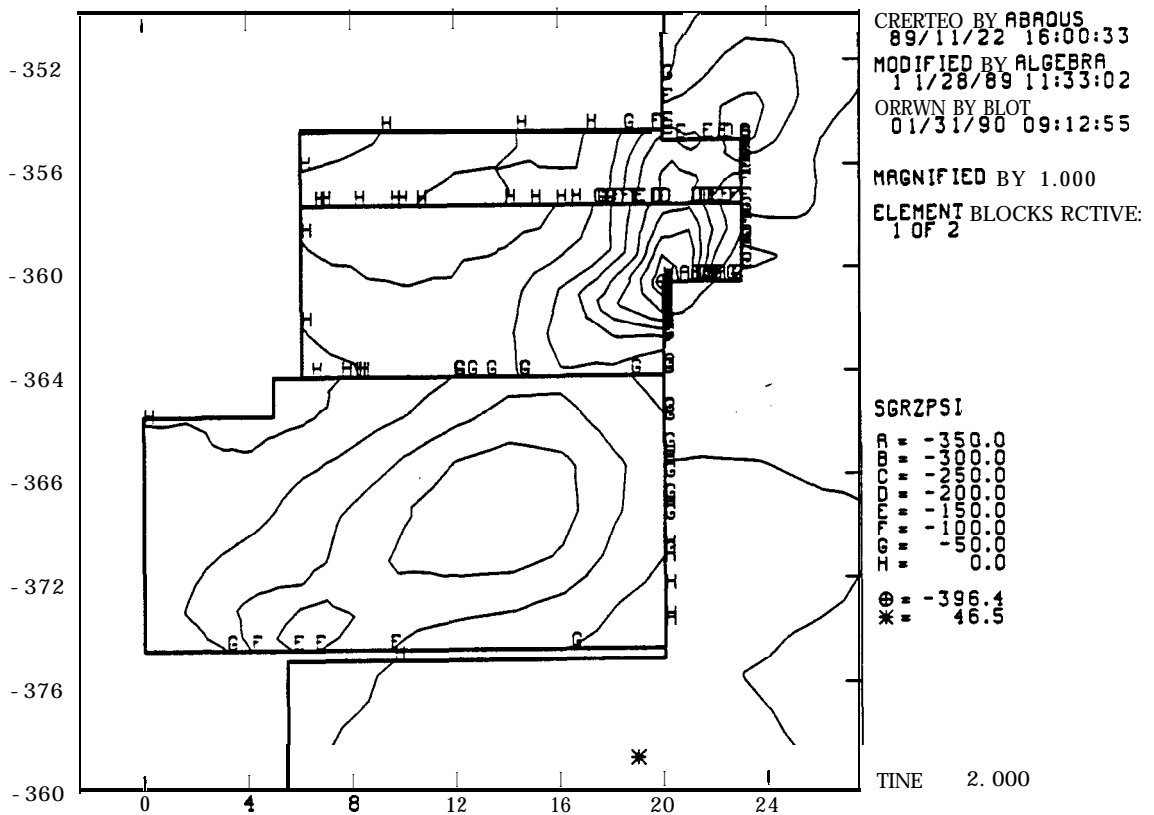

Figure 4.7. Contours of Shear Stress (SGRZPSI) in Service Shaft Bulkhead

5. Markel Incline Bulkhead

The Markel incline has a nominal 16 x 24-foot cross section, sloping upwards towards the north at 7". A 21-foot section of the drift was widened 10 feet in all directions in preparation for pouring the 36 x 44-foot bulkhead. The bulkhead was installed in three parts, as shown in Figure 5.1. Because the bulkhead is not in a vertical shaft, reference to "upper" and "lower" bulkhead sections is not appropriate. Instead, we will use the terms "outer" and "inner" in relation to the oil storage area, with the outer surface of the Markel bulkhead corresponding to the upper surface of the other bulkheads. "Horizontal" and "vertical" will be used to indicate the x- and y-directions in the plane of the bulkhead; the z-direction normal to the bulkhead surface is designated "axial."

5.1 Model

Because of its rectangular cross section, the Markel bulkhead is not well approximated using axisymmetric or planar two-dimensional assumptions. Therefore a three-dimensional model of the bulkhead and surrounding salt was necessary. Taking advantage of two planes of symmetry along the axis of the drift, the size of the problem was reduced by analyzing only one-fourth of the domain. As described in Section 2.2, the center of the outer bulkhead has been removed, leaving a rectangular annulus of concrete resting against the outer shoulder of the salt. The inner bulkhead has been translated forward so that it is in contact with the outer annulus.

A preliminary mesh of 2238 nodes and 1325 linear-displacement elements was constructed as an analysis check and to serve as a reference for adequacy of the mesh refinement. The second and final mesh, shown in Figure 5.2, doubled the resolution in all three directions. This mesh had just over 13,000 nodes and 10,000 linear-displacement brick elements. As in the analyses of the other bulkheads, the far-field boundaries were constrained against displacement normal to the boundary. The factors of safety calculated using the two meshes agreed within 5 percent, indicating that the mesh refinement is indeed adequate.

This configuration was analyzed using ABAQUS. Eight-node brick C3D8 elements were used in the salt and concrete regions, and INTER4 interface elements were used between the salt and concrete and between the upper and lower bulkheads. All the INTER4 elements were assigned a friction coefficient of 0.1. The salt was initialized with a compressive normal stress of 100 psi in all directions.
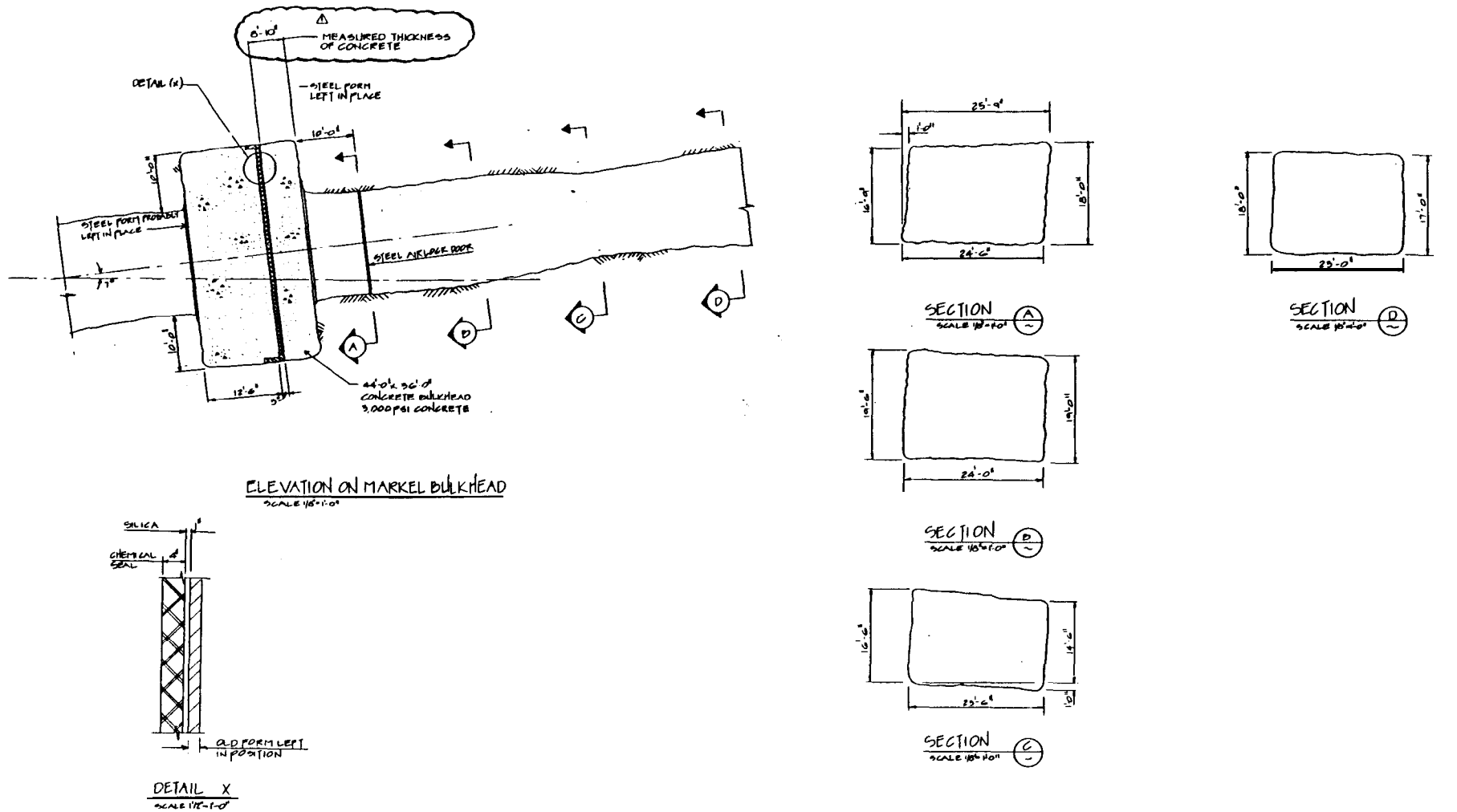
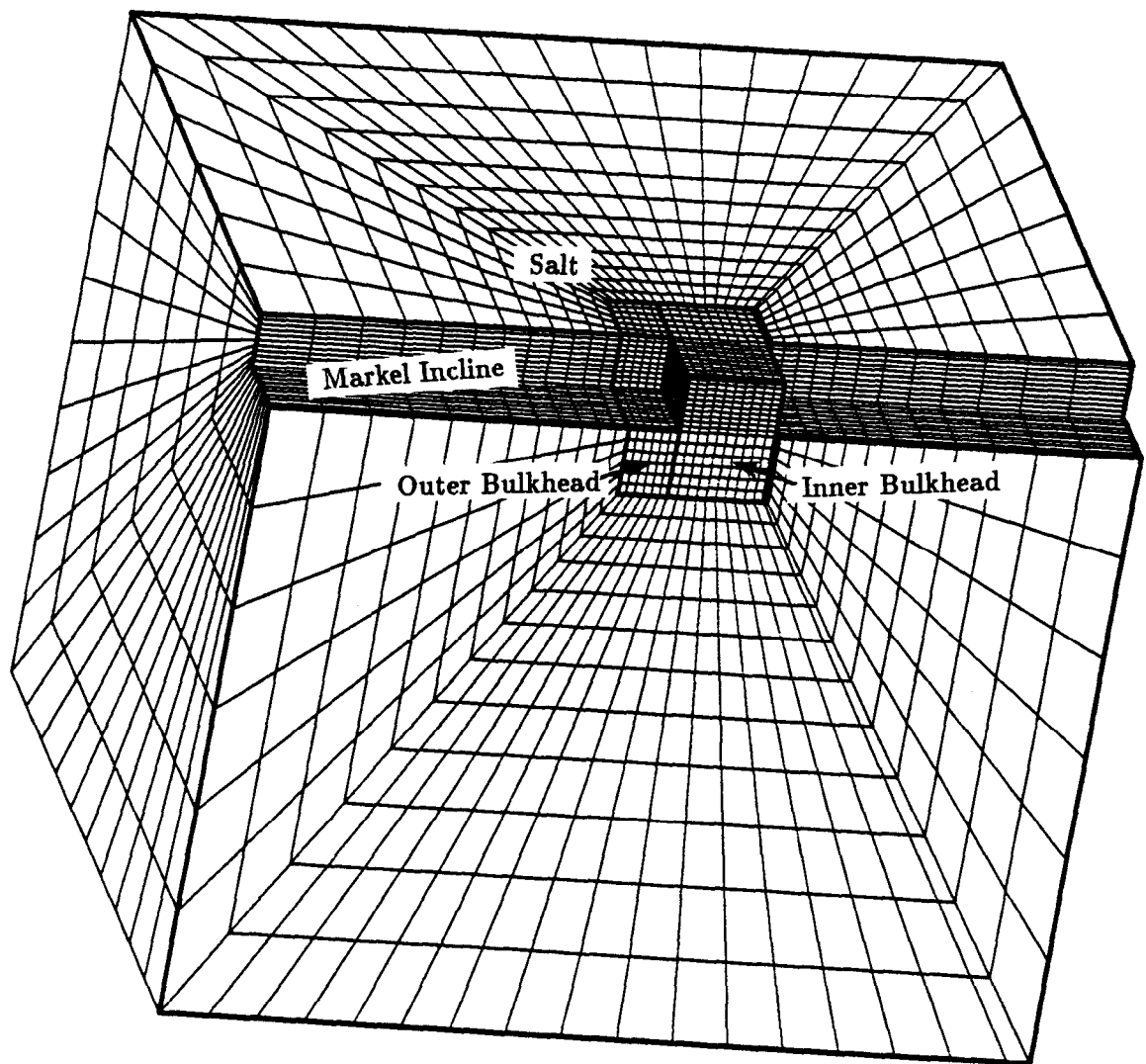**Figure 5.1.** As-Built Drawing of Markel Incline Bulkhead

Labels in figure: Salt, Markel Incline, Outer Bulkhead, Inner Bulkhead

Figure 5.2. Mesh Used in Analyzing the Markel Incline Bulkhead

5.2 Results

The first load step was solved for equilibrium resulting from the initially-stressed salt relaxing toward the drift and the bulkhead. No flooding pressure was applied in this load step. A plot of the deformed mesh in the vicinity of the bulkhead is shown in Figure 5.3. Deformations have been magnified 200 times to aid in visualization. Note that the salt has not only closed in toward the drift, but has also deformed axially toward the bulkhead. Again, the apparent penetration of the salt into the inner surface of the bulkhead is merely an artifact of exaggerating the displacements to this extreme. The average horizontal pressure exerted by the salt onto the perimeter of the lower bulkhead in the first load step was found to be 95 psi; the average vertical pressure was 105 psi.

For the second load step, flooding pressure of 267 psi was applied to the back surface of the inner bulkhead and all exposed faces of the salt behind the bulkhead. Figure 5.4 shows the deformations resulting from the final loading, again magnified 200 times for visualization purposes.

The most severe stress is the horizontal stress (σ_x) due to bending of the bulkhead whose contours are shown in Figure 5.5. Its maximum, indicated by the star, occurs at the center of the outer surface of the inner bulkhead. At this point σ_x is also the maximum principal stress. Profiles of the horizontal, vertical, and axial stresses through the thickness of the bulkhead are shown in Figure 5.6. These values are calculated at the element centers for the row of elements nearest the axial centerline of the bulkhead. Axial compressive stresses vary from 2.5 psi near the free surface to 263 psi near the flooded surface. Horizontal stresses due to bending range from 174 psi tension to 383 psi compression; the vertical stresses due to bending lie in the range 151 psi tension to 344 psi compression. When extrapolated to the free surface at the center of the bulkhead, the calculated horizontal tensile stress reaches a maximum of 215 psi. Compared to the concrete's assumed direct tensile strength of 461 psi, this represents a safety factor of 2.1.
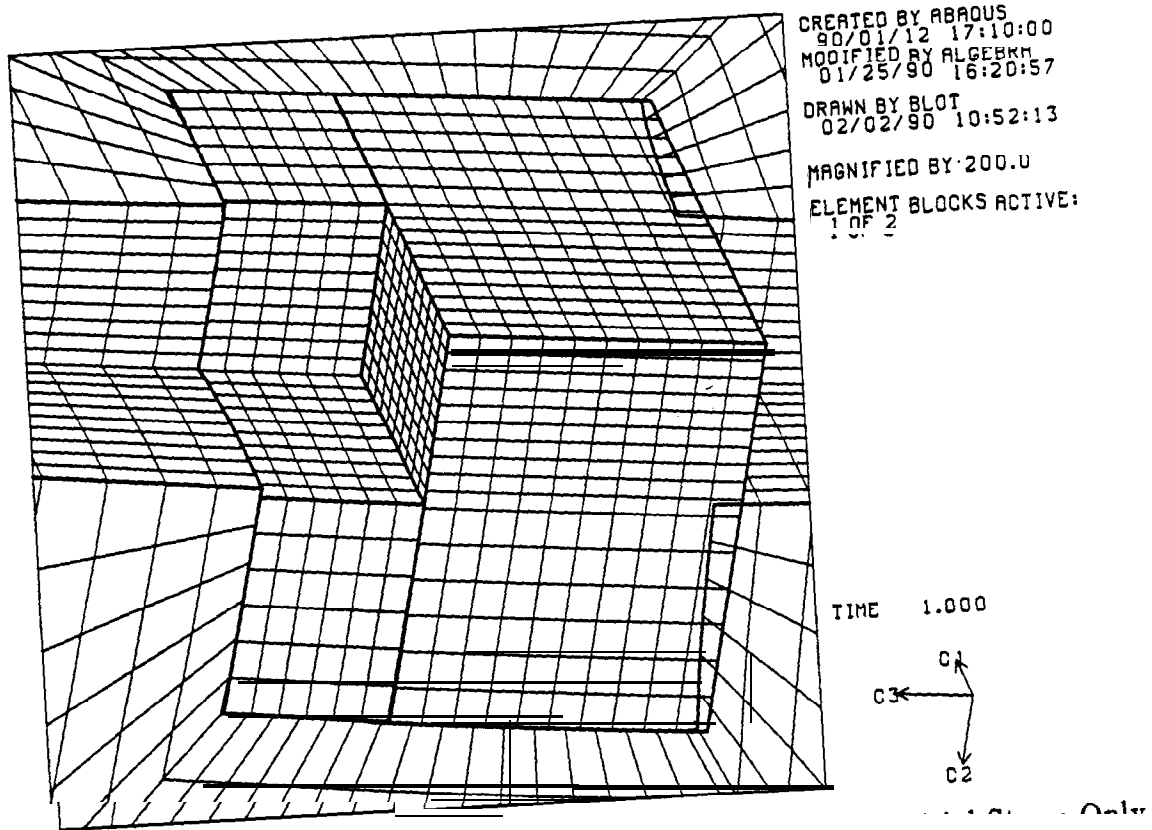
Figure 5.3. Deformed Mesh of Markel Bulkhead Response to Initial Stress Only
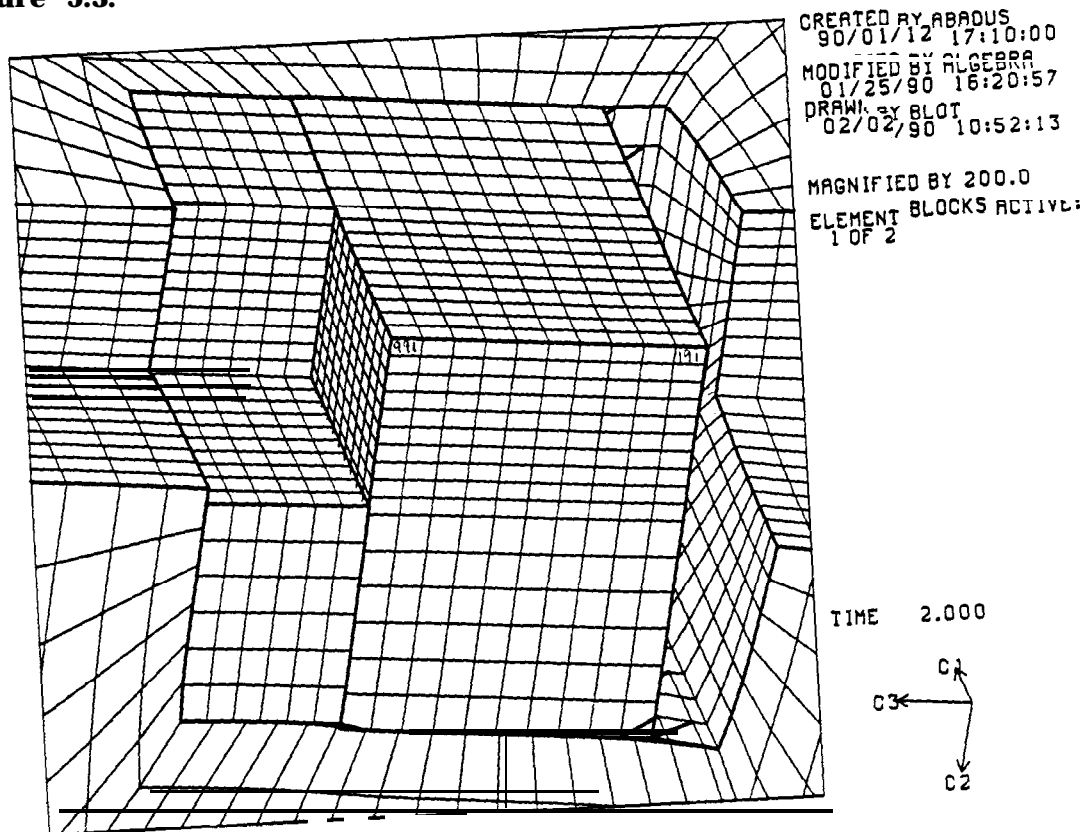
Figure 5.4. Deformed Mesh of Markel Bulkhead Response to Final Load

35

CREATED BY ABAQUS
90/01/12 17:10:00
MODIFIED BY ALGEBRA
01/25/90 16:20:57
DRAWN BY BLOT
02/02/90 10:52:13

MAGNIFIED BY 1.000

ELEMENT BLOCKS ACTIVE:
1 OF 2

SIGXPSI

A = -350.0
B = -250.0
C = -150.0
D = -50.0
E = 50.0
F = 150.0

⊕ = -402.3
✳ = 174.0

TIME   2.000

Figure 5.5. Contours of Horizontal Normal Stress (SIGXPSI) in Markel Incline Bulkhead

Figure 5.6. Variation of Horizontal, Vertical, and Axial Stress through the Thickness of the Markel Incline Bulkhead

36

6. Raisebore Bulkheads

Bulkheads in the two raisebores are nearly identical to each other, but they differ from the production shaft bulkhead, the service shaft bulkhead, and the Markel bulkhead in that they have neither a key nor an overhang of salt to prevent uplift from flooding of the storage area. Instead, they are held to the salt by lateral rows of rockbolts (see Figures 6.1 and 6.2). Each bulkhead is composed of an upper and a lower bulkhead section with each section 16 ft in diameter. The lower bulkhead section is five feet thick and rests on an annular shoulder above the 6-ft-diameter borehole. The upper bulkhead section is four feet eight inches thick and rests on a four-inch thick layer of CSR which separates it from the lower bulkhead. The upper bulkhead is held in place by three rows of 24 No. 14 rock bolts, each having a cross-sectional area of 2.25 inches (nominally 1.75 inches in diameter). The lower bulkhead is restrained by two such rows of rockbolts.

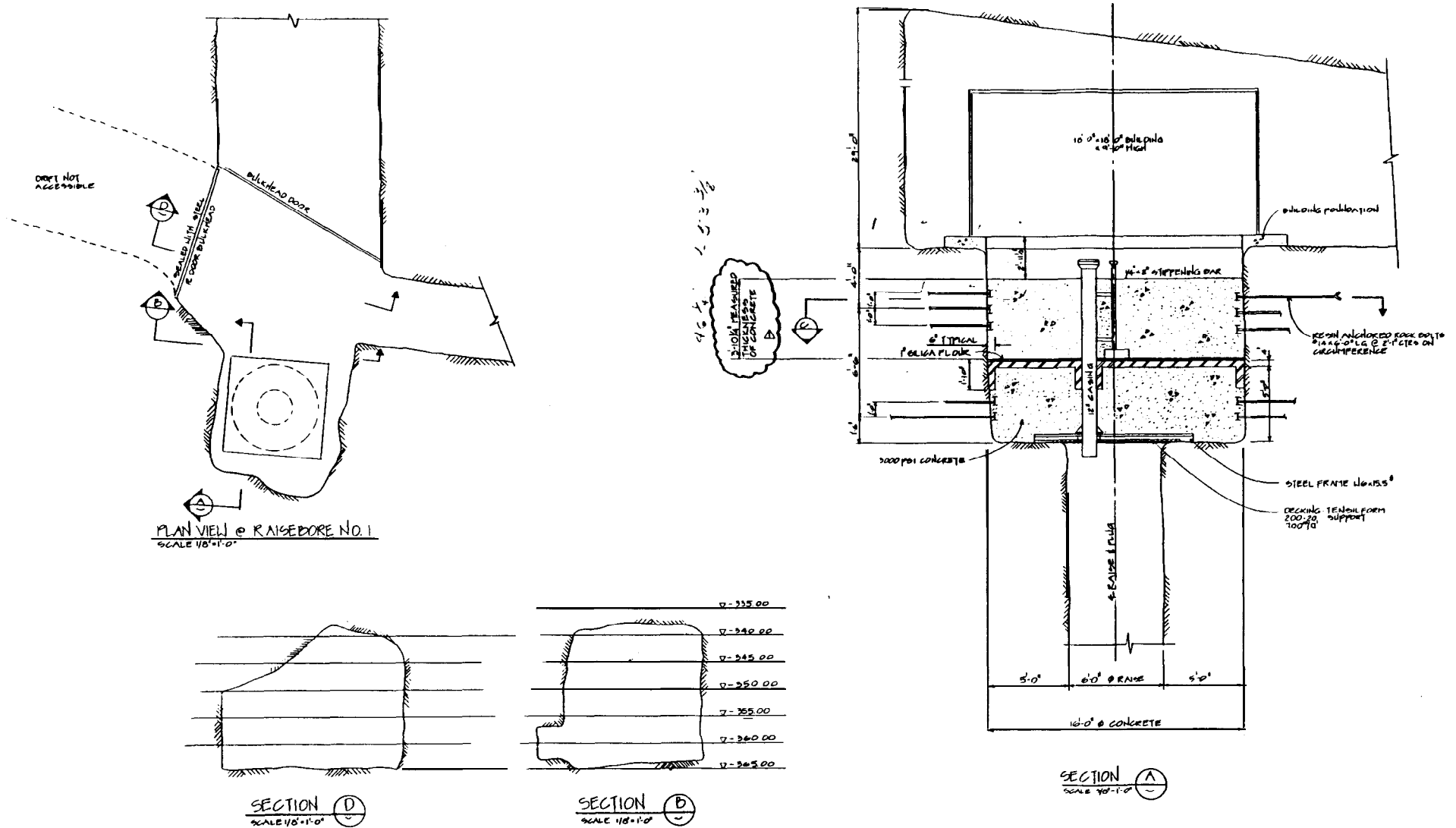Because of the similarity of these two bulkheads, a single model that contains features common to both bulkheads was used in the analysis. The more severe flooding pressure of 245 psi on Raisebore No. 2 was used as a conservative loading condition.

The analysis was complicated by the fact that, as shown below, the capacity of the lower section of the bulkhead to contain flood pressures depends crucially on the capacity of the upper section to contain the CSR pressure between the bulkhead sections.

A further complication arose because the upper section had been demonstrated to be capable of containing 200 psi of CSR pressure, even though such pressure was expected to cause cracking, depending on the amount of in situ stress applied by the formation. In fact, cracking had been observed on the surface of the upper bulkhead section. If the cracks extend through the thickness of the upper bulkhead, the cohesion of the cross-linked CSR polymer presumably prevents the seal material from flowing through the cracks. Discussion of the pressure beyond which the upper bulkhead can no longer contain the CSR becomes part of the calculation of factor of safety.

The complexity of the relation between the upper and lower bulkheads is related to the enhancement of the pressure in the CSR that would occur as a flood pressure lifts the lower bulkhead off of its shelf. Upward motion of the lower bulkhead would further compress the CSR and cause an increase in CSR pressure that both pushes down on the lower bulkhead and raises the upper bulkhead. Even for a specified flooding pressure from below, the *net* pressure acting on the lower bulkhead *must* be calculated.

To address the complex nature of this problem, analytic descriptions of its mechanics were deemed more appropriate than for the other bulkheads. The derived expressions for this problem were also more tractable than for the other bulkheads because shear along

PLAN VIEW @ RAISEBORE NO. 1
SCALE 1/8"=1'-0"

SECTION D
SCALE 1/8"=1'-0"

SECTION B
SCALE 1/8"=1'-0"

SECTION A
SCALE 1/8"=1'-0"

Jacobs Engineering Group Inc.
CENTRAL REGION   HOUSTON, TEXAS

Strategic
Petroleum
Reserve

DOE SPR FACILITY
WEEKS ISLAND   LA.

AS BUILT DRAWING OF NO. 1
6'-0" ∅ BOREHOLE BULKHEAD

WI-C-201-SK-1008

Figure 6.1.   As-Built Drawing of Bulkhead in Raisebore No. 1

Figure 6.2. As-Built Drawing of Bulkhead in Raisebore No. 2

interfaces is less intricately a part of this problem than it is for the others. Still, it was necessary to add some simplifying assumptions to make the analysis manageable. These simplifications are:

1. Both the upper and lower halves of the bulkhead are treated as thin plates. This is conservative in that it ignores both the added shear stiffeness associated with thick plates and the radial constraint that the boundaries impose on crack opening of thick plates.

2. The possibility that the upper bulkhead may be pre-cracked is ignored when computing its stiffness in bending. The upper bulkhead may actually have a lower bending stiffness than the model suggests, and in this regard the model may not be conservative. If the analysis indicates an acceptable overall safety factor, then this assumption will have to be re-examined.

3. The bulkheads are taken to be simply supported at the boundaries. This is conservative since the multiple layers of rock bolts should in fact serve to reduce rotation at the boundaries and reduce the bending moment throughout the bulkhead.

4. The upper bulkhead is taken to be capable of sustaining 200 psi CSR pressure.

Because the failure modes discussed in Chapter 2 are manifested differently in this bulkhead than in the other bulkheads, they are restated here in the context of the raise-bore bulkheads. Two sorts of failure mode are considered: bending failure of the concrete and shear failure of the rockbolts.

1. The bulkhead fails if a crack forms in the lower bulkhead. This is a conservative assumption, since initiation of a crack in the bulkhead does not necessarily lead to escape of oil from the storage cavern.

2. The rockbolts fail through shear if the net vertical load on a bulkhead is greater than that which would fail the rockbolts when each of the bolts in a bulkhead section carries equal shear stress. The uniform stress assumption reflects a redistribution of stress amongst the bolts due to salt creep.

6.1 Calculation of Loads on Each Bulkhead Section

Three specific sources of failure are examined for each combination of initial and loaded conditions in calculating the factor of safety.

1. What is the shear stress in the bolts of the upper bulkhead?

2. What is the maximum tensile stress in the lower bulkhead due to bending?

3. What is the shear stress in the bolts of the lower bulkhead?

Evaluation of all of the above requires calculation of the incremental change in CSR presssure with deflections due to flooding.

The displacement field Aw occurring in a thin, simply-supported, circular plate subject to a uniform pressure increment Ap is given by Timoshenko [10]:

$$\Delta w(r, \Delta p) = \Delta p \frac{R^2 - r^2}{64D} \left(\frac{5 + \nu}{1 + \nu} R^2 - r^2 \right) \tag{6.1}$$

Here $D = \frac{1}{12} E h^3 / (1 - \nu^2)$ is the plate rigidity, ν is the Poisson ratio of the plate material, R is the radius of the plate, E is Young's modulus, and h is the plate thickness.

Integration of this expression over the area of the plate yields the net **volume** swept out by the deformed plate:

$$\Delta V(\Delta p) = Ap \frac{0.0982(\nu + 7)R^6}{6D(\nu + 1)} \tag{6.2}$$

For the upper bulkhead, this becomes

$$\Delta V_{\text{upper}} = (1.29 \text{ in}^3/\text{psi}) \Delta p_{\text{CSR}} \tag{6.3}$$

and for the lower bulkhead it becomes

$$\Delta V_{\text{lower}} = (1.047 \text{ in}^3/\text{psi})(\Delta p_{\text{CSR}} - p_{\text{flood}}) \tag{6.4}$$

Of course, the above equation applies only if the net pressure on the lower bulkhead acts upward, $(p_{\text{flood}} > p_{\text{CSR}})$ so that bulkhead is lifted off the salt lip-this is the case that applies in all failure modes of interest. The difference in the coefficients in these two expressions is due to the difference in thickness of the two bulkhead halves.

The net increase in the CSR cavity will be that due to the flexure of both plates:

$$\Delta V_{\text{CSR}} = (1.29 + 1.047)(\text{in}^3/\text{psi}) \Delta p_{\text{CSR}} - 1.047(\text{in}^3/\text{psi}) p_{\text{flood}} \tag{6.5}$$

The pressure increase on the CSR boundaries due to a volume decrease in the CSR cavity is calculated using the bulk modulus of the CSR (1.4×10^5 psi).

$$\Delta p_{\text{CSR}} = -1.4 \times 10^5 \text{ psi} \times \Delta V_{\text{CSR}} / V_0 \tag{6.6}$$

The initial volume V_0 of the CSR is calculated from the geometry of the cavity to be $V_0 = 2.0 \times 10^5 \text{ in}^3$, yielding

$$\Delta V_{\text{CSR}} = -1.43(\text{in}^3/\text{psi}) \Delta p_{\text{CSR}} \tag{6.7}$$

Combining Equations 6.7 and 6.5 for the volume change of the CSR cavity, an equation is obtained for the increase in the CSR pressure in terms of the storage cavern flood pressure.

$$\Delta p_{CSR} = 0.28 p_{flood} \tag{6.8}$$

In summary, when a flood pressure p_{flood} is applied to the bottom of the lower bulkhead, the pressure in the cavity will be

$$p_{CSR} = \hat{p}_{CSR} + 0.28 p_{flood} \tag{6.9}$$

where $\hat{p}_{CSR}$ is the initial CSR pressure. It is these pressures which are used in calculating the effective loads on the upper and lower bulkheads.

6.2 Calculation of Stresses in Bulkheads and Rockbolts

The maximum tensile stress occurring in a thin, simply-supported, circular plate subject to a uniform pressure p is also given by Timoshenko [10]:

$$\sigma_{max}(p) = \frac{3(3 + \nu)R^2}{8h^2} p \tag{6.10}$$

To this formula we must superimpose the in situ radial stress σ_{insitu} transferred to the bulkhead from the surrounding salt. In the finite-element analyses of the other bulkheads, this confining pressure ranged from 92 to 105 psi. Because of the proximity of the rooms immediately above the raisebore bulkheads, however, a more conservative value of 80 psi was used here. The maximum stress found in the lower plate when subject to flooding is then

$$
\begin{aligned}
\sigma_{max}(p) &= \frac{3(3 + 0.18)8^2}{8 \times 5^2}(p_{flood} - p_{CSR}) + \sigma_{insitu} \\
&= 3.05(p_{flood} - p_{CSR}) + \sigma_{insitu} \\
&= 2.2\, p_{flood} - 3.05\, \hat{p}_{CSR} + \sigma_{insitu}
\end{aligned}
\tag{6.11}
$$

The corresponding factor of safety, using a failure stress of 461 psi for concrete, is

$$F_s(\text{bending of lower bulkhead}) = \frac{461 \text{ psi}}{2.2\, p_{flood} - 3.05\, \hat{p}_{CSR} + \sigma_{insitu}} \tag{6.12}$$

The shear stress in the bolts on each bulkhead is also easily calculated (net force over net area):

$$\tau = \frac{\pi R^2 p}{N_{bolts/row} \times N_{rows} \times A_{bolt}} \tag{6.13}$$

With 3 rows of 24 bolts per row, the shear stress in the bolts on the upper bulkhead is

$$
\begin{aligned}
\tau_{upper} &= \frac{\pi(8 \times 12)^2}{24 \times 3 \times 2.25} p_{CSR} \\
&= 179 p_{CSR} \\
&= 50 p_{flood} + 179 \hat{p}_{CSR}
\end{aligned}
\tag{6.14}
$$

Table 6.1. Factors of Safety in the Raisebore Bulkheads for a Range of Initial CSR Pressures

		Factors of Safety		
		Bending Failure of Lower B.H.	Shear Failure of Upper B.H.	Shear Failure of Lower B.H
Initial	0	1.00	4.41	1.14
CSR	100	2.99	1.79	2.64
Pressure	200	N/A	1.12	N/A

Similarly, the shear stress in the bolts on the lower bulkhead $(N_{\text{rows}} = 2)$ is

$$\tau_{\text{lower}} = \frac{\pi(8 \times 12)^2}{24 \times 2 \times 2.25}(p_{\text{flood}} - p_{\text{CSR}})$$
$$= 268 \times (p_{\text{flood}} - p_{\text{CSR}})$$
$$= 193 p_{\text{flood}} - 268 \hat{p}_{\text{CSR}} \qquad (6.15)$$

The corresponding factors of safety, using a shear strength of 54,000 psi, are

$$F_s(\text{shear of upper bulkhead bolts}) = 54 \times 10^3 \text{psi}/(50 p_{\text{flood}} + 179 \hat{p}_{\text{CSR}}) \qquad (6.16)$$

and

$$F_s(\text{shear of lower bulkhead}) = 54 \times 10^3 \text{psi}/(193 p_{\text{flood}} - 268 \hat{p}_{\text{CSR}}) \qquad (6.17)$$

Table **6.1** reports the factors of safety for each failure mechanism for a flooding pressure of 245 psi and various initial values of CSR pressure. If the CSR layer is initially unpressurized, **a** bending failure of the lower bulkhead is likely to occur. For the higher values of initial CSR pressure, the upper bulkhead is increasingly likely to experience shear failure in the bolts. For a 200 psi initial CSR pressure, the flooding pressure of 245 psi raises the CSR pressure to 269 psi, so that there is no net uplift pressure acting on the lower bulkhead. Therefore, the factor-of-safety equations are not applicable to the lower bulkhead in this case.

For the full range of possible initial CSR **pressurizations,** there occurs at least one failure mechanism with an appreciably low factor of safety. Implicit in all of the above is that the upper bulkhead can contain the CSR pressure involved in each calculation. There can be no certainty that it can contain any more than the 200 psi that has been measured. However, the factors of safety calculated in consideration of other failure mechanisms indicate that the bulkhead needs to be upgraded, so the conclusions about the vulnerability of the bulkheads is not affected by this uncertainty.

7. Conclusions

Five bulkheads in the Weeks Island SPR facility have been analyzed to predict their capacity to withstand pressure from a worst-case flooding scenario, that of flooding from within the oil storage caverns. In all but the raisebore bulkheads, a conservative approach was taken when choosing model parameters and simplifying assumptions. The conservative assumptions for these finite-element calculations include

- a low estimate of the compressive strength of the concrete used in the bulkheads

- lack of any pressure restraint on the CSR layer from the upper bulkhead

- the presumption of failure upon *initiation* of cracking in the lower bulkhead section

- a low estimate of the frictional resistance between the bulkhead and the surrounding salt.

These assumptions are repeated here to emphasize that the analyses represent lower bounds on the factors of safety in these bulkheads.

The conservatism of assigning any tensile strength at all to unreinforced concrete may perhaps be questioned. Without any tensile strength, however, one would be obliged to perform a post-cracked, zero-tension nonlinear analysis of the bulkheads. Such an analysis was beyond the scope of this study. It was the consensus of both analysis teams that a linear-elastic concrete model using a nominal tensile strength would provide an adequate basis for the rework decision.

Under the assumptions made, we have found that the service shaft bulkhead would be near its load-carrying capacity in the event of the postulated flood. Bulkheads in the Markel incline and production shaft, on the other hand, exhibit the capacity to withstand at least two and three times the postulated loads, respectively.

Closed-form analysis of the two raisebore bulkheads indicates that the most likely failure mechanism depends on the initial pressure in the CSR material. Whatever that initial pressure, however, some part of the bulkhead would be close to failure if the postulated flood were to occur.

References

[1] Overview *of Underground Construction, Weeks Island Storage Site, New Iberia, Louisiana,* Prepared for Petroleum Operations and Support Services, Inc. by PB-KBB Inc., New Orleans, LA, June 1982.

[2] Ortiz, T. *S., Strategic Petroleum Reserve (SPR) Geological Summary Report, Weeks Island Salt* Dome, SAND80-1323, Sandia National Laboratories, Albuquerque, NM, October 1980.

[3] *Conceptual Design Report for Bulkhead Upgrades,* Prepared for the US DOE Strategic Petroleum Reserve by Jacobs Engineering Group, Houston, TX, 1988.

[4] Linn, J.K. and K. Thirumalai, *A Summary Report on the Results of the First Technical Meeting Between Sandia and STI on the Stability of Ezisting Bulkheads in Weeks Island SPR Site,* Science and Technology Institute, Fairfax, VA, August 31, 1989.

[5] Lunn, R. E., "Bulkhead Concrete Strengths," memorandum to J. K. Linn at Sandia National Laboratories, from Jacobs Engineering Group Inc., Houston, TX, August 21, 1989

[6] Blanford, M. L., "Resolution of Discrepancies in Analyses of Weeks Island Production Shaft Bulkhead," memorandum to J. K. Linn, Sandia National Laboratories, Albuquerque, NM, November 30, 1989.

[7] Wawersik, W. R., "Friction Coeffecients Governing End Constraints In Laboratory Compression Tests," accepted for publication in *International Journal of Rock Mechanics and Mining Sciences.*

[8] Chen, W. F., *Plasticity in Reinforced Concrete,* McGraw-Hill, New York, NY, **1982,** p. 26.

[9] *ABAQUS User's Manual, Version 4.7,* Hibbitt, Karlsson & Sorensen, Inc., Providence, RI, 1988.

[10] Timoshenko, S., and S. Woinowsky-Krieger, *Theory* of *Plates and Shells, 2nd Ed.,* McGraw-Hill, New York, NY, 1959.

Distribution:

U.S. DOE SPR PMO (11)
900 Commerce Road East
New Orleans, LA 70123
Attn: D. R. Spence, PR-62
     L. J. Rousseau, PR-621.3
     E. E. Chapple, PR-622 (5)
     D. W. Whittington, PR-622
     J. C. Kiiroy, PR-631.2
     TDCS (2)

U.S. Department of Energy (1)
Strategic Petroleum Reserve
1000 Independence Avenue SW
Washington, D.C. 20585
Attn: R. Smith

U.S. Department of Energy (1)
Oak Ridge Operations Office
P.O. Box E
Oak Ridge, TN 37831
Attn: W. Manning

Boeing Petroleum Services (3)
850 South Clearview Parkway
New Orleans, LA 70123
Attn: T. Eyermann
     J. Siemers
     K. Wynn

Jacobs Engineering Group, Inc. (1)
P.O. Box 53495
Houston, TX 77081
Attn: Bill Luhn

Science and Technology Institute, Inc. (3)
P.O. Box 729
Fairfax, VA 22030
Attn: K. Thirumalai
     B. Dendrou
     A. R. Ingraffea

Raymond D. Krieg
Engineering Science and Mechanics Dept.
301 Perkins Hall
The University of Tennessee
Knoxville, TN 37996-2030

Sandia Internal:

1510 J. W. Nunziato
1520 L. W. Davison
1521 H. S. Morgan
1521 M. L. Blanford (10)
1521 D. J. Segalman
1521 J. G. Arguello
1522 R. C. Reuter
1523 J. H. Biffle
1524 D. R. Martinez
1530 J. R. Asay
1550 C. W. Peterson
3141 S. A. Landenberger (5)
3141-1 C. L. Ward (8)
     For DOE/OSTI
3151 W. I. Klein (3)
6000 D. L. Hartley
6200 V. L. Dugan
6250 P. J. Hommert
6257 J. K. Linn (10)
6257 J. T. Neal
6257 R. L. Parrish
6257 J. L. Todd, Jr.
6258 J. G. Castle
8524 J. A. Wackerly

48